International Journal of Bifurcation and Chaos, Vol. 9, No. 7 (1999) 1393–1424

EXPERIMENTAL STUDY OF IMPULSIVE SYNCHRONIZATION OF CHAOTIC AND HYPERCHAOTIC CIRCUITS

MAKOTO ITOH
Department of Information and Communication Engineering, Fukuoka Institute of Technology, 3-30-1, Wajiro-Higashi, Higashi-Ku, Fukuoka 811-0295, Japan

TAO YANG and LEON O. CHUA
Department of Electrical Engineering and Computer Sciences, University of California at Berkeley, Berkeley, CA 94720, USA

Received January 15, 1999; Revised March 22, 1999

In this paper, experimental results on impulsive synchronization of two kinds of chaotic circuits; namely, Chua's oscillator and a hyperchaotic circuit, are presented. To impulsively synchronize two Chua's oscillators, synchronization impulses sampled from *one* state variable of the driving circuit are transmitted to the driven circuit. To impulsively synchronize two hyperchaotic circuits, synchronizing impulses sampled from *two* signals of the driving circuit are sent to the driven circuit. Our experimental results show that the accuracy of impulsive synchronization depends on both the period and the width of the impulse. The ratio between the impulse width and impulse period for "almost-identical" *synchronization* increases as the impulse period increases. The robustness of impulsive synchronization to additive noise is also experimentally studied. For sufficiently short impulse periods, no significant differences are observed between impulsive and continuous synchronizations. The performance of chaotic spread spectrum communication systems based on impulsive synchronization is also studied experimentally.

1. Introduction

Over the past ten years, a number of interesting chaotic spread spectrum communication systems had been proposed [Halle *et al.*, 1992; Parlitz, *et al.*, 1992; Kocarev *et al.*, 1992; Dedieu *et al.*, 1993; Parlitz *et al.*, 1994; Itoh & Murakami, 1995; Lipton & Dabke, 1996; Yang & Chua, 1997a, 1997b, 1997c, 1998a, 1998b; Itoh, 1999]. In the usual setting of chaotic spread spectrum communication systems, the message signals are modulated by chaotic spreading signals and then the spreaded signals are transmitted to receivers. An identical synchronization between the chaotic system in the transmitter and that in the receiver [Pecora & Carroll, 1990] is needed for recovering the chaotic spreading signal at the receiver end. Therefore, "synchronization" is the most important requirement for designing chaotic spread spectrum communication systems.

Recently, a new synchronization scheme called *impulsive synchronization* was developed [Yang & Chua, 1997a, 1997c]. In impulsive synchronization only samples of state variables (or functions of state variables) called *synchronization impulses* are used to synchronize two chaotic systems. The bandwidth or time slot needed to transmit synchronization signals is dramatically reduced in impulsive synchronization when compared to continuous synchronization. Impulsive synchronization had been applied to several chaotic spread spectrum secure

communication systems, and had exhibited good performance [Yang & Chua, 1997a, 1997b, 1997c, 1998a, 1998b; Itoh, 1999]. In secure communication systems based on impulsive synchronization the transmitted signal consists of a sequence of time frames. Each time frame has a length of T seconds and consists of two regions. The first region, which has a length of Q seconds, is a synchronization region consisting of synchronization impulses. The synchronization impulses are used to impulsively synchronize the chaotic systems in both the transmitter and the receiver. The second region, which has a length of $T - Q$ seconds, contains the scrambled message signal. Since Q is usually very small compared to T, the loss of time in packing the message signal is negligible [Yang & Chua, 1997a, 1997c].

From the experimental point of view, it is not so easy to synchronize two actual chaotic circuits by using impulsive synchronization in view of the following reasons:

- In actual circuits, noise is unavoidable.
- Parameter mismatch and changes (drifts) in the component parameters of the chaotic circuits in the transmitter and the receiver are unavoidable.
- The width of the impulse Q cannot be chosen to be too small, especially when the circuits are hyperchaotic, because noise and parameter mismatch will soon desynchronize the chaotic circuits even though the two circuits have synchronized during the period when synchronization impulses are present.

The first experimental results on impulsive synchronization were presented in [Panas *et al.*, 1998]. In that experiment, two Chua's oscillators were effectively synchronized by using narrow impulses ($Q/T = 0.16\%$, $1/T = 18000$ Hz). To apply the impulsive synchronization to chaotic communication systems, we need to perform more detailed experiments and carry out performance analysis on the following aspects of impulsive synchronization.

- Examine impulsive synchronization under a wide frequency range and noisy channels.
- Evaluate the minimum length of Q and the ratio of Q to T; namely, Q/T.
- Apply impulsive synchronization to hyperchaotic circuits.

In this paper, we experimentally study the performance of impulsive synchronization of two kinds of chaotic circuits: Chua's oscillator and a hyperchaotic circuit [Matsumoto *et al.*, 1986]. To impulsively synchronize two Chua's oscillators, we transmit impulses sampled from one state variable of the driving circuit to the driven circuit. To impulsively synchronize two hyperchaotic circuits, we transmit impulses sampled from two signals of the driving circuit to the driven circuit. In both cases, the synchronization impulses are transmitted through one communication channel. We have also evaluated the minimum length of the interval Q for achieving almost-identical synchronization under a different impulse period T. We have experimentally verified the promising performances of impulsive synchronization in different chaotic spread spectrum communication systems, in which Chua's oscillators and the hyperchaotic circuits were used to generate spreading signals. The performance of digital chaotic spread spectrum communication systems in noisy channels was also studied in our experiments.

In Sec. 2, we present experimental results on the impulsive synchronization of Chua's oscillators and hyperchaotic circuits. In Sec. 3, experimental results on different chaotic spread spectrum communication systems based on impulsive synchronization are given. Some concluding remarks are presented in Sec. 4.

2. Experimental Results

In this section, we present our experimental results on the impulsive synchronization between two Chua's oscillators and two hyperchaotic circuits. We report the minimum impulse width Q and the ratio Q/T for achieving impulsive synchronization under different impulse frequencies. We also add small noise to the driving signals and examine the robustness of the impulsive synchronization to additive noise.

2.1. *Impulsive synchronization of Chua's oscillators*

The dynamics of Chua's oscillator [Madan, 1993], whose block diagram is shown in Fig. 1, are given by the following state equation:

$$C_1 \frac{dv_1}{dt} = \frac{v_2 - v_1}{R} - f(v_1)\,, \tag{1}$$

$$C_2 \frac{dv_2}{dt} = \frac{v_1 - v_2}{R} + i\,, \tag{2}$$

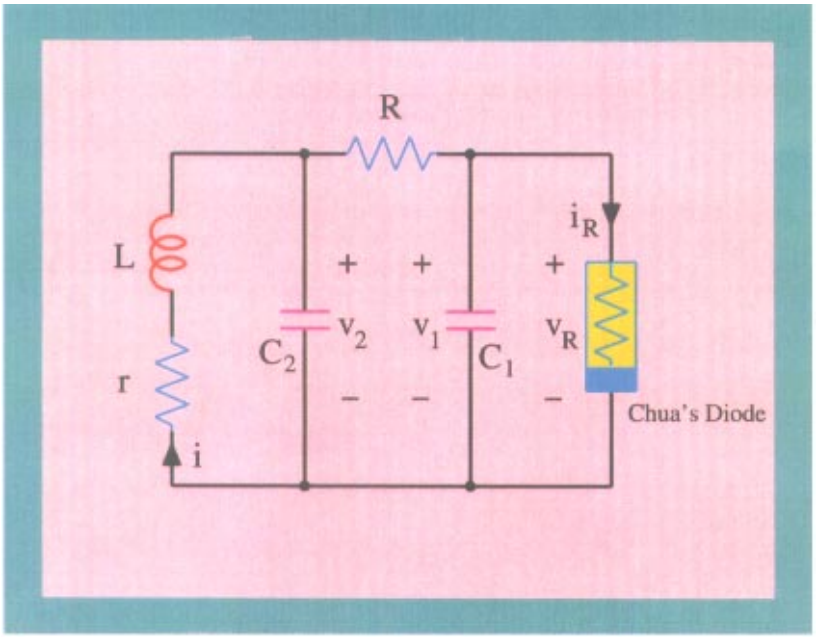

Fig. 1. Circuit diagram of Chua's oscillator.

$$L\frac{di}{dt} = -v_2 - ri\,, \tag{3}$$

where $f(\cdot)$ is the nonlinear characteristic of Chua's diode shown in Fig. 1, defined by

$$f(v_1) = G_b v_1 + \frac{1}{2}(G_a - G_b)(|v_1 + E| - |v_1 - E|)\,, \tag{4}$$

where E is the breakpoint voltage of Chua's diode. The parameters for Chua's oscillators used in our experiments are given by:

$$C_1 = 10.3 \text{ nF}, \quad C_2 = 99.6 \text{ nF}\,,$$
$$L = 22.3 \text{ mH}, \quad R = 885\ \Omega\,, \tag{5}$$
$$r = 68.9\ \Omega, \quad G_a = -0.875 \text{ mS}\,,$$
$$G_b = -0.516 \text{ mS}, \quad E = 0.78 \text{ V}\,. \tag{6}$$

Different projections of the experimentally observed Chua's double scroll attractor are shown in Fig. 2.

The experimental setting for the impulsive synchronization between two Chua's oscillators is shown in Fig. 3. Chua's oscillators #1 and #2 are the driving circuit and the driven circuit respectively. The voltage buffer is used to set up a unidirectional coupling from Chua's oscillator #1 to Chua's oscillator #2. The switch is implemented by a CMOS IC (4066BP) chip, which is controlled by a binary(on/off) signal called the *switching signal*. The parameter mismatch between two Chua's oscillators is within 0.5%. In the experimental setting shown in Fig. 3 the voltage v_1 of Chua's oscillator #1 is chosen as the driving signal. The sequence of synchronization impulses and the corresponding switching signals are shown in Fig. 4. Observe that the switching signal has a "high" voltage level and a "low" voltage level. When the switching signal is in the "high" voltage level, the switch shown in Fig. 3 is turned on and a synchronization impulse is transmitted to the driven circuit. When the switching signal is in the "low" voltage level, the switch shown in Fig. 3 is turned off and the two Chua's oscillators are separated electronically.

When we observe the synchronized state from an oscilloscope, we feed one state variable of the driving circuit into the X-axis input of the oscilloscope and the corresponding state variable of the driven circuit into the Y-axis input. If a 45-degree line appears on the screen, then synchronization is achieved [Pecora & Carroll, 1990; Chua *et al.*, 1992, 1993; Panas *et al.*, 1998]. Figures 5(a)–5(c) show the oscilloscope traces of the synchronized states on the v_1–v_1' plane, v_2–v_2' plane, and i–i' plane, respectively. Since a current cannot directly be fed into the inputs of an oscilloscope, we feed the voltages $r_1 i$ and

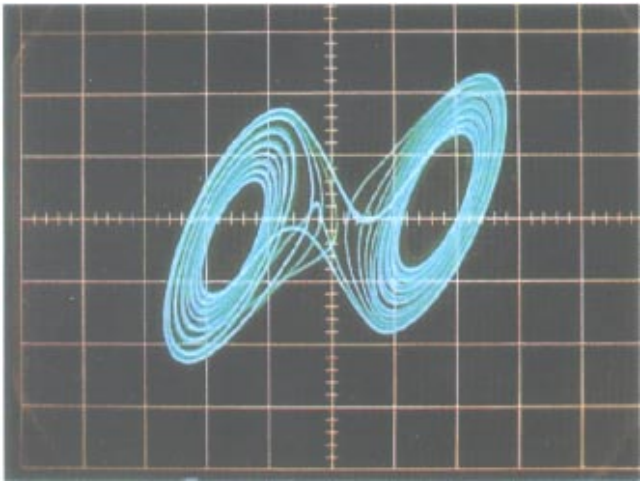

(a)

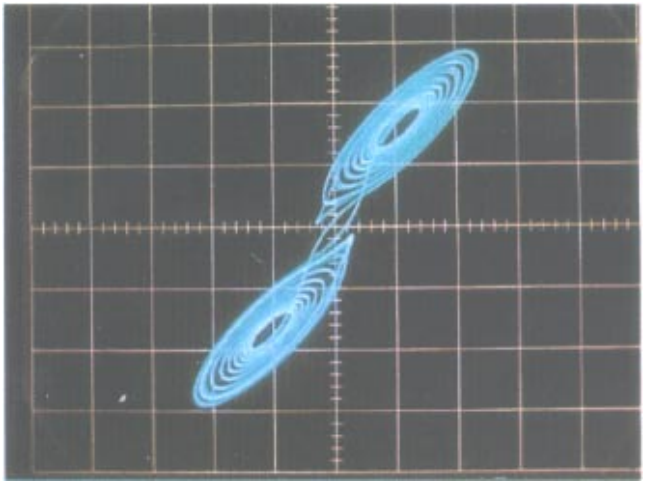

(b)

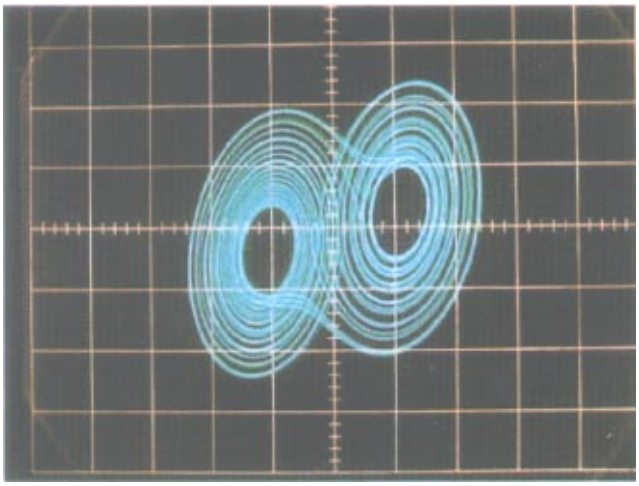

(c)

Fig. 2. Observed strange attractor of Chua's oscillator used in our experiments. (a) Projection of Chua's double scroll attractor onto the (v_1, v_2)-plane. (b) Projection of Chua's double scroll attractor onto the (v_1, i)-plane. (c) Projection of Chua's double scroll attractor onto the (v_2, i)-plane.

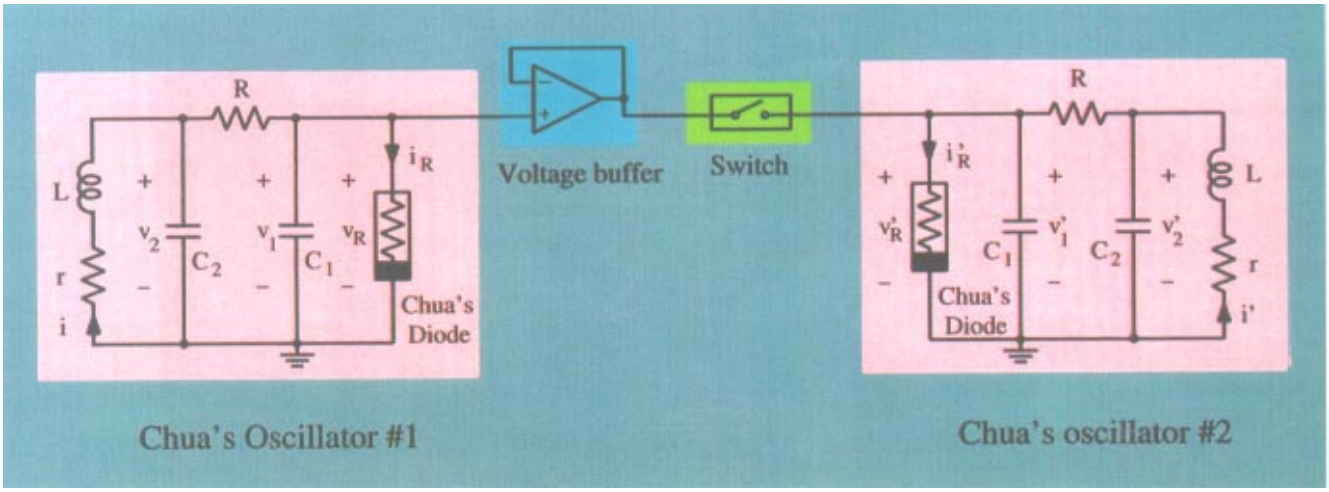

Fig. 3. Circuit diagram of impulsive synchronization between two Chua's oscillators.

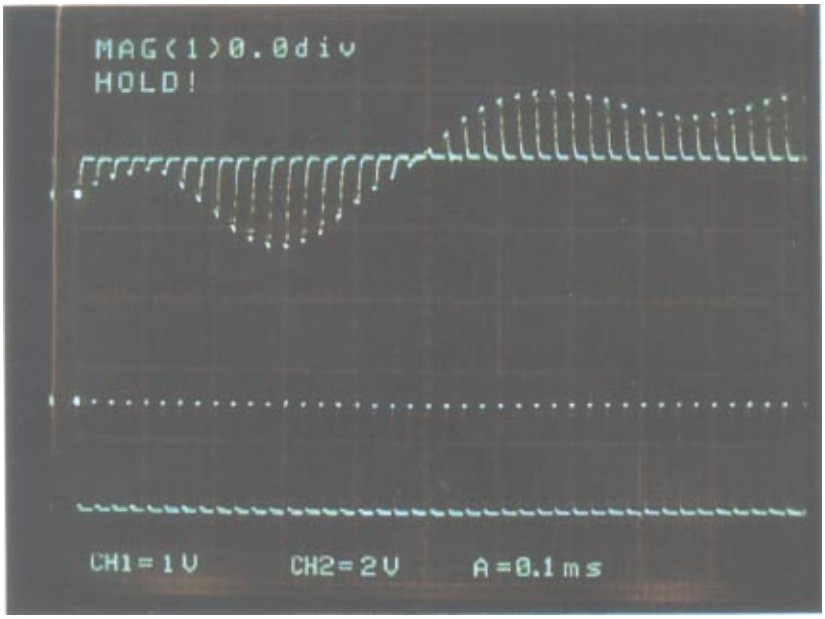

(a)

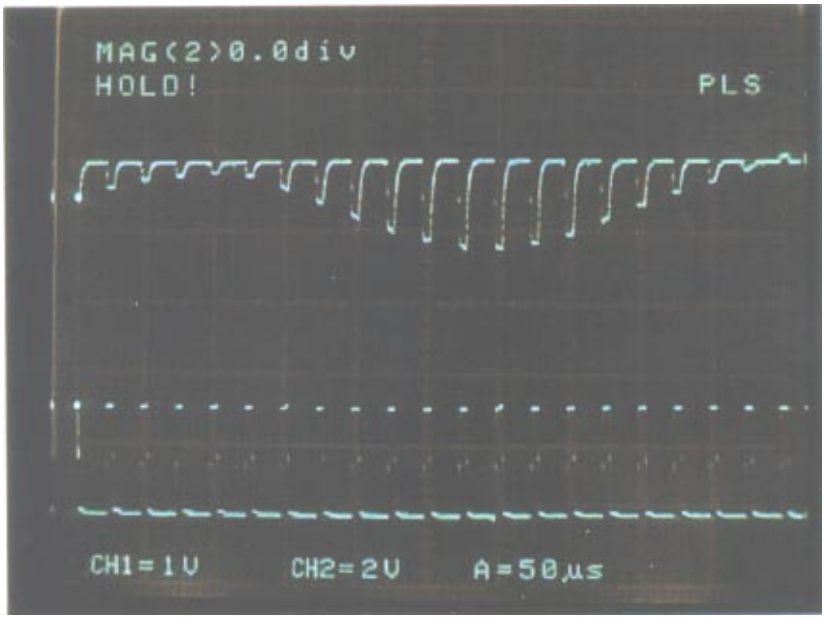

(b)

Fig. 4. (a) The sequence of synchronization impulses (the upper trace with vertical scale 1 V/div) and switching signal (the lower trace with vertical scale 2 V/div). The horizontal scale is 0.1 ms/div. (b) Details of the sequence of synchronization impulses (the upper trace) and switching signal (the lower trace). The vertical scales for both channels are the same as those in (a). The horizontal scale is 0.1 μs/div.

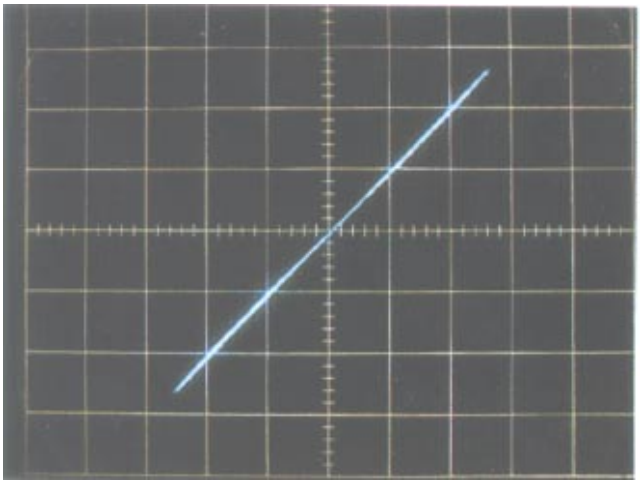

(a)

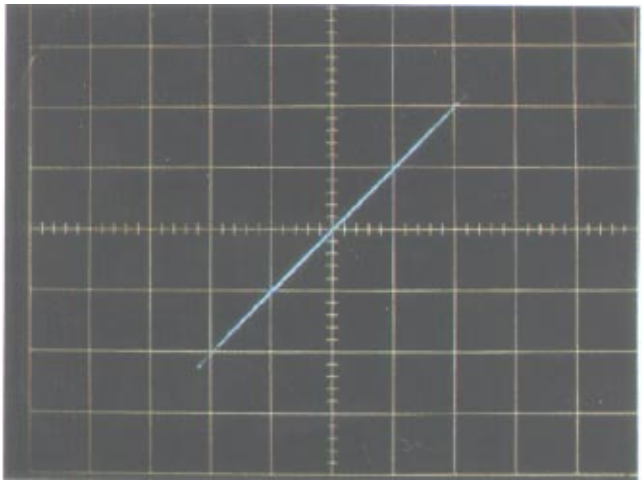

(b)

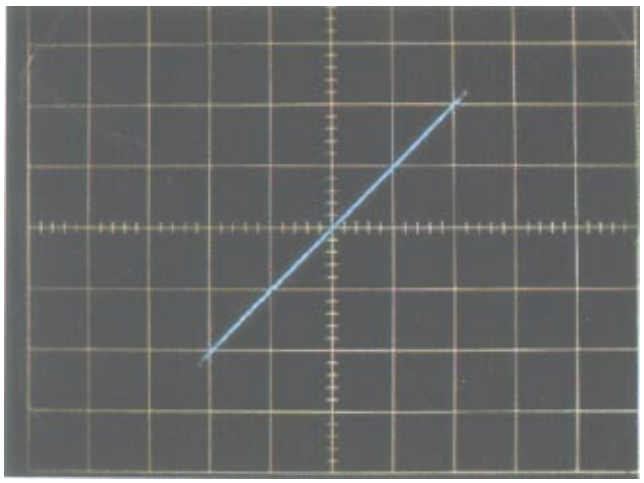

(c)

Fig. 5. Experimental results of the almost-identical synchronization between two Chua's oscillators with $Q = 6.4 \times 10^{-7}$ s and $T = 8.0 \times 10^{-6}$ s. (a) Oscilloscope trace of v_1 versus v_1'. (b) Oscilloscope trace of v_2 versus v_2'. (c) Oscilloscope trace of i versus i'.

$r_1 i'$ to display the tracing on the i–i' plane.[1] The experimental conditions are $Q = 0.64 \times 10^{-6}$ s and $T = 8.0 \times 10^{-6}$ s. Observe that an *almost-identical synchronization*[2] is achieved.

Two main factors can affect the performance of impulsive synchronization: the minimum impulse width for achieving synchronization, denoted by Q, and the frame length T. The experimental results are summarized in Fig. 6. Figure 6(a) shows the relation between Q and T. Observe that the relationship is almost linear except for the region when T is below 1×10^{-4} s. We enlarged the region within the black box as shown in Fig. 6(b). To show more details, we enlarged the region within the black box in Fig. 6(b) as shown in Fig. 6(c), which is almost piecewise-linear. Figure 6(d) shows the relation between Q and the frequency of impulses $F \stackrel{\triangle}{=} 1/T$. Figure 6(e) shows the relation between Q/T and T. Observe that Q/T is approximately equal to a small constant when T is small, and a big constant when T is large. Correspondingly, we show the relation between Q/T and F in Fig. 6(f). The

[1] In our experimental circuits, the resistor r is divided into two resistors $r_1 = 30.0\ \Omega$ and $r_2 = 38.9\ \Omega$.

[2] An almost-identical synchronization is defined by the following conditions:
(1) The 45-degree line on the oscilloscope screen is sufficiently thin.
(2) No significant distortion is found along this 45-degree line.
The experimental results can depend strongly on the measuring instruments and circuit components.

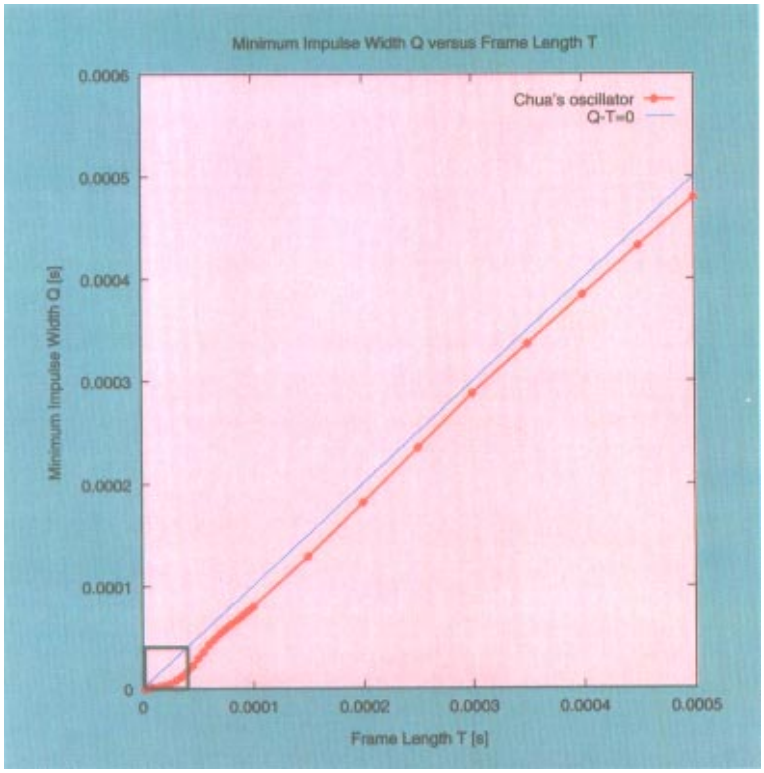

(a)

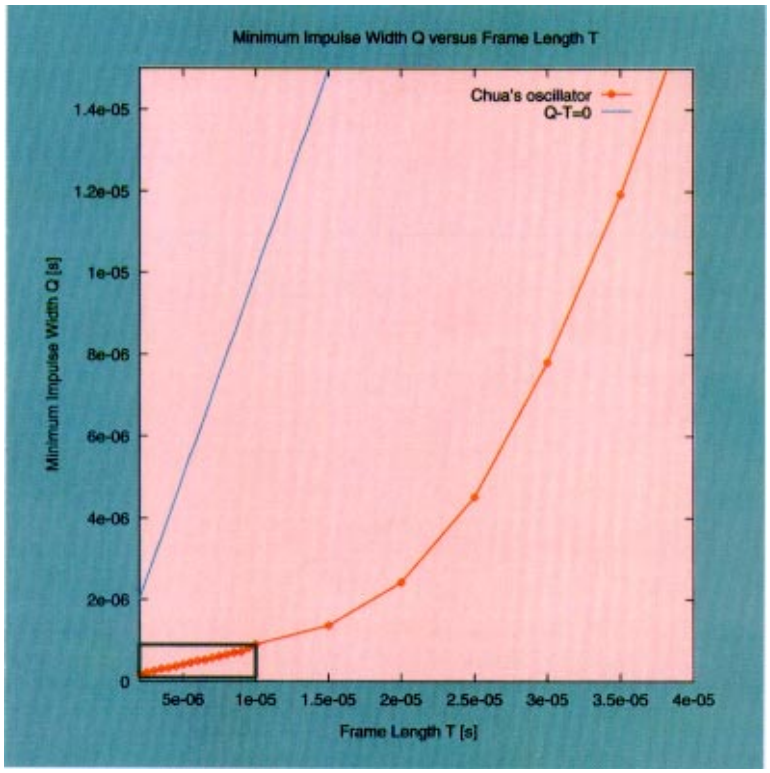

(b)

Fig. 6. The relationship between the minimum impulse width Q for achieving an almost-identical synchronization of two Chua's oscillators and the frame length T, or frequency of impulses $F = 1/T$. (a) Q versus T from 0 to 5×10^{-4} s. The upper straight line $Q = T$ is shown for comparison purpose. (b) Q versus T from 0 to 4×10^{-5} s. (c) Q versus T (over the range of 2×10^{-6} s $\leq T \leq 1 \times 10^{-5}$ s). (d) Q versus frequency F. (e) Ratio Q/T versus T. (f) Ratio Q/T versus frequency F.

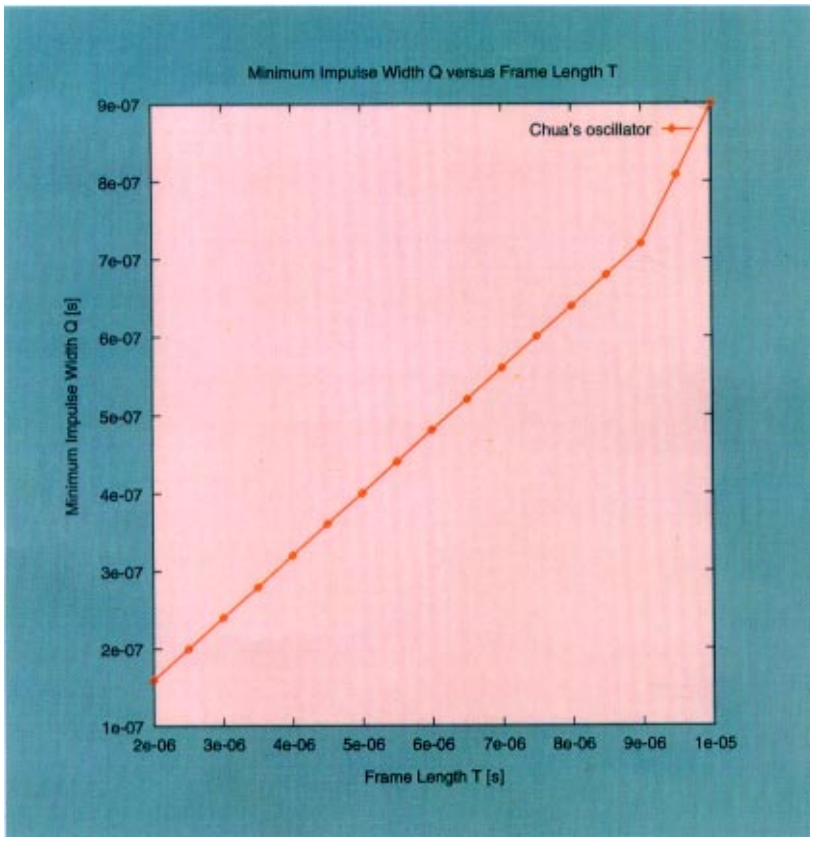

(c)

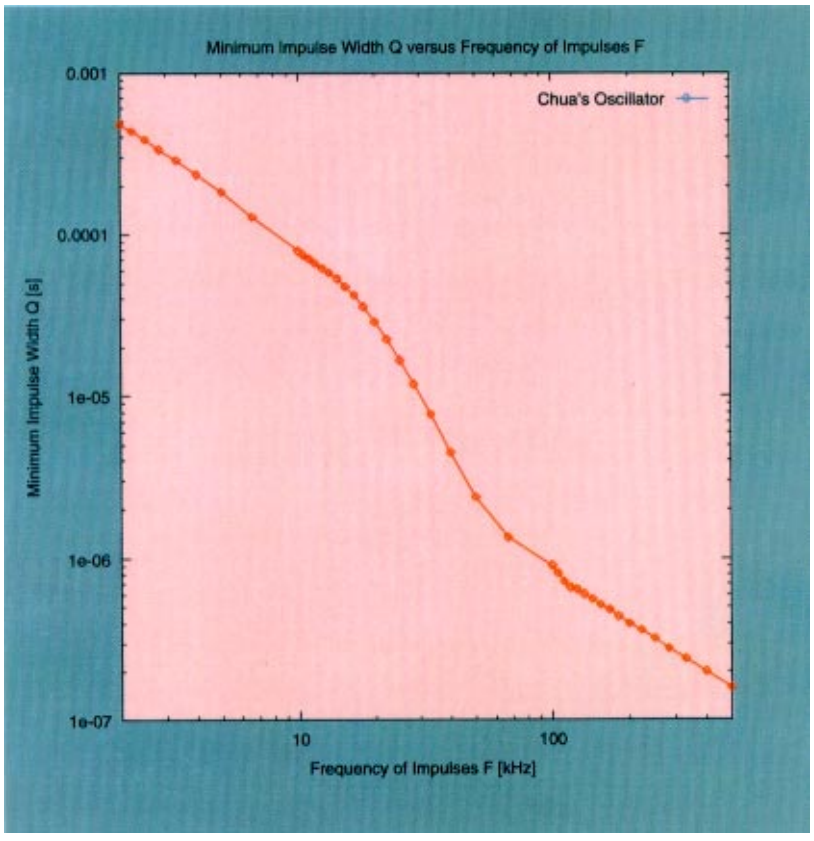

(d)

Fig. 6. (*Continued*)

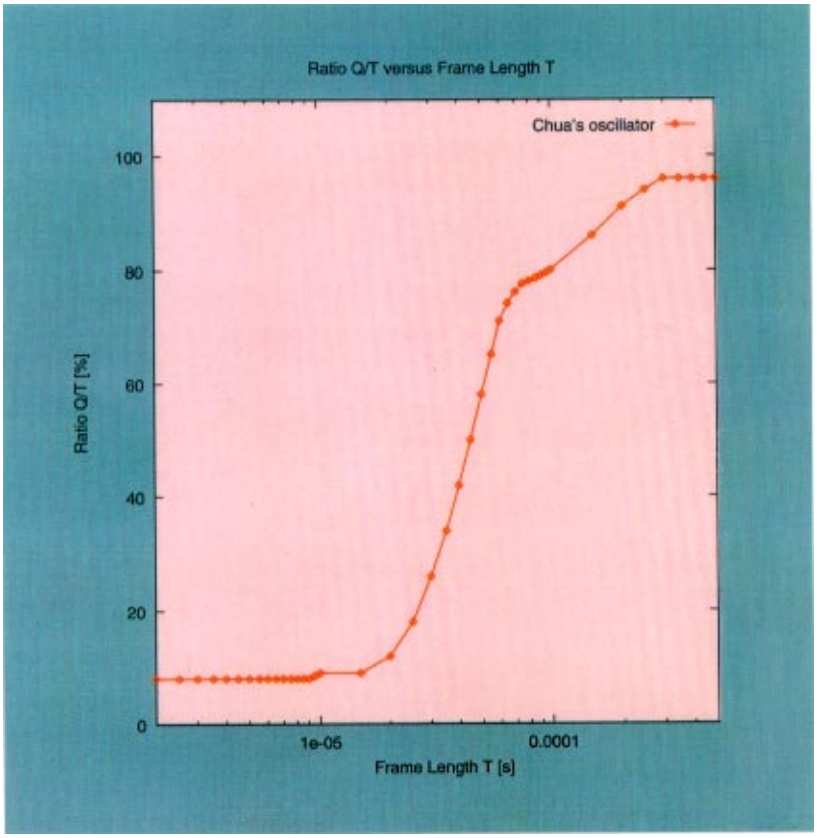

(e)

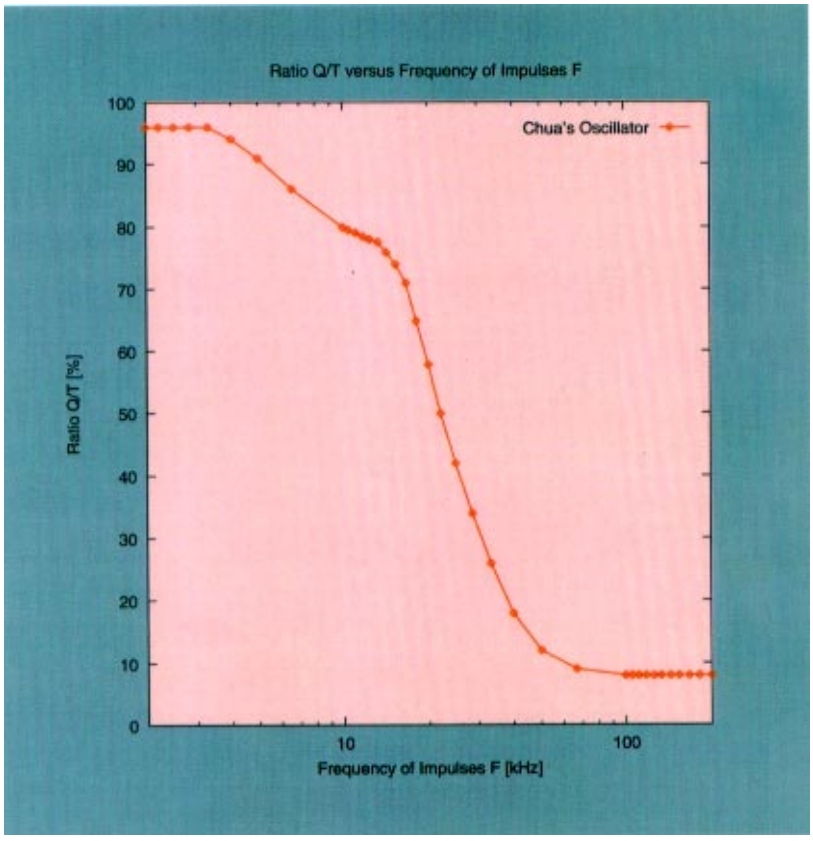

(f)

Fig. 6. (*Continued*)

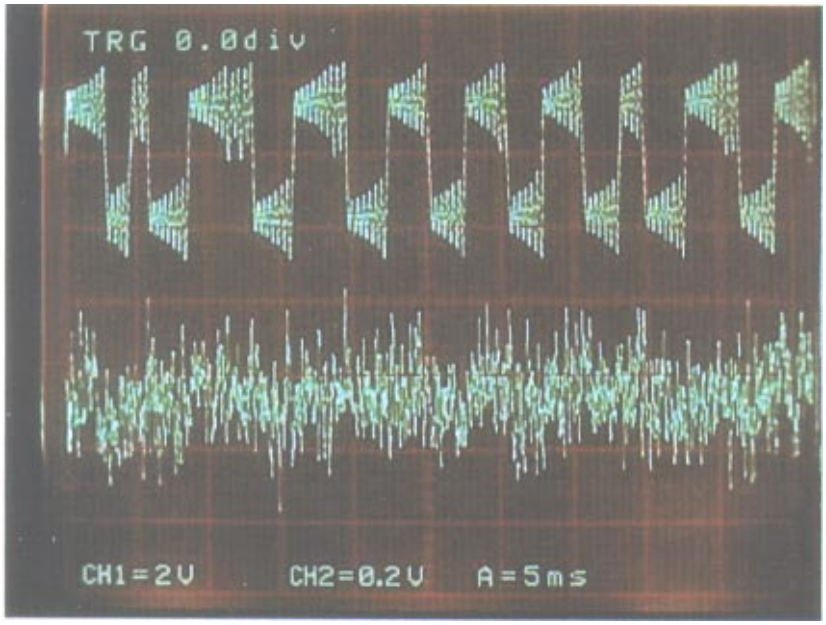

Fig. 7. The transmitted signal v_1 and the additive noise. Vertical scales are 2 V/div for the upper trace and 0.2 V/div for the the lower trace. Horizontal scale is 5 ms/div.

following conclusions can be drawn from our experimental observations.

(1) For $T \leq 9.0 \times 10^{-6}$ s

To achieve an almost-identical synchronization, the impulse width occupies only 8% of the impulse period and the remaining 92% of the time period is therefore available for transmitting scrambled signals. In this case, Q increases in proportion to the length of T. Therefore, we can make Q sufficiently small with respect to T, as shown in [Yang & Chua, 1997a, 1997b; Itoh, 1999].

(2) For 9.0×10^{-6} s $\leq T \leq 5.0 \times 10^{-5}$ s

The ratio Q/T increases from 8% to 50% as T increases. The available time interval for transmitting scrambled signals decreases.

(3) For 5.0×10^{-5} s $\leq T \leq 5.0 \times 10^{-3}$ s

To achieve an almost-identical synchronization, the impulse width occupies at least 50% of the impulse period. Therefore, Q cannot be chosen sufficiently small with respect to T.

We then added noise[3] to the driving signal and examined the robustness of the impulsive synchronization to additive noise. The additive noise is shown in Fig. 7. Observe that the amplitude range of the noise is approximately 1/10 of that of v_1. In our experiments, the noise is added after the switch. The experimental results are shown in Figs. 8–10 with $T = 5.0 \times 10^{-6}$ s. Figures 8(a)–8(c) show the oscilloscope traces on the v_1–v_1' planes with $Q/T = 8\%$, 50% and 100%, respectively. Figures 9(a)–9(c) show the oscilloscope traces on the v_2–v_2' planes with $Q/T = 8\%$, 50% and 100%, respectively. Figures 10(a)–10(c) show the oscilloscope traces on the i–i' planes with $Q/T = 8\%$, 50% and 100%, respectively. There is no observable difference between impulsive synchronization and continuous synchronization because in Figs. 9 and 10 the thickness of the 45-degree lines for impulsive synchronization and for continuous synchronization is almost the same. Thus, the impulsive synchronization is robust to small additive noise. Furthermore, we conjecture that more accurate circuit components may be chosen to make Q much shorter.

2.2. *Impulsive synchronization of hyperchaotic circuits*

The block diagram of the hyperchaotic circuit used in our experiments are shown in Fig. 11 [Matsumoto

[3]FM receivers tuned at frequency 106 MHz are used to generate noise. No commercial radio station broadcasts in the frequency band around 106 MHz.

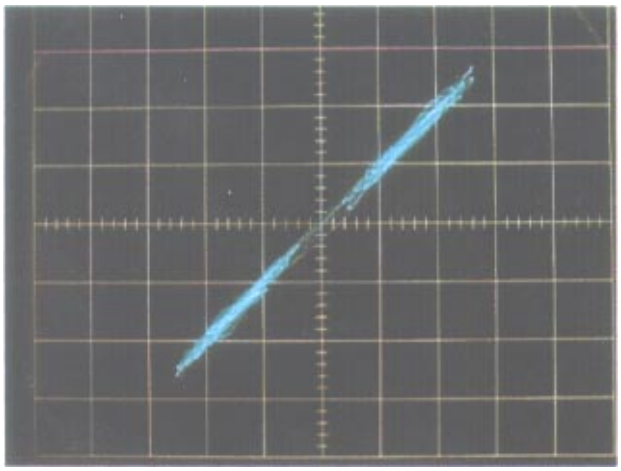

(a)

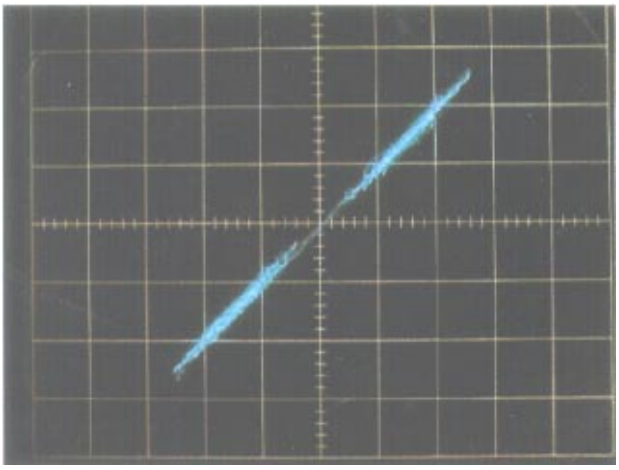

(b)

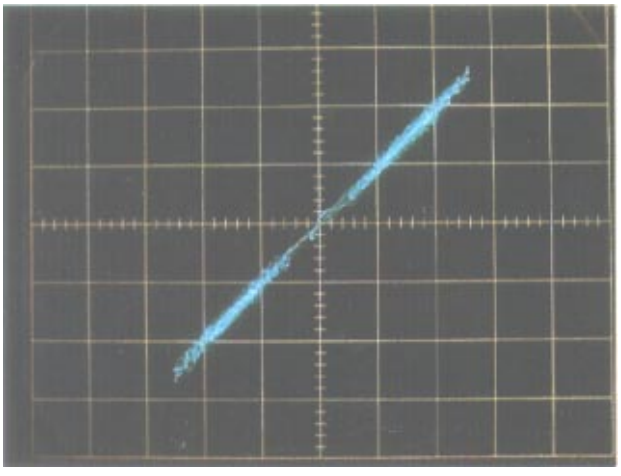

(c)

Fig. 8. Robustness of impulsive synchronization between Chua's oscillators to additive noise under the condition $T = 5.0 \times 10^{-6}$ s. Oscilloscope traces on the v_1–v_1' planes are shown. (a) Q/T is equal to 8%. (b) Q/T is equal to 50%. (c) Q/T is equal to 100%. This condition is equivalent to continuous synchronization.

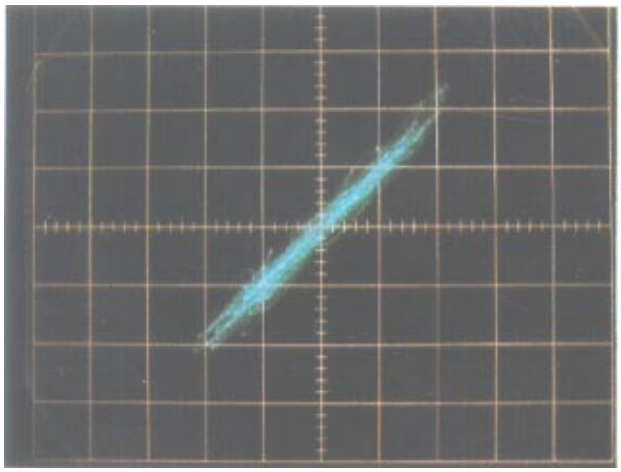

(a)

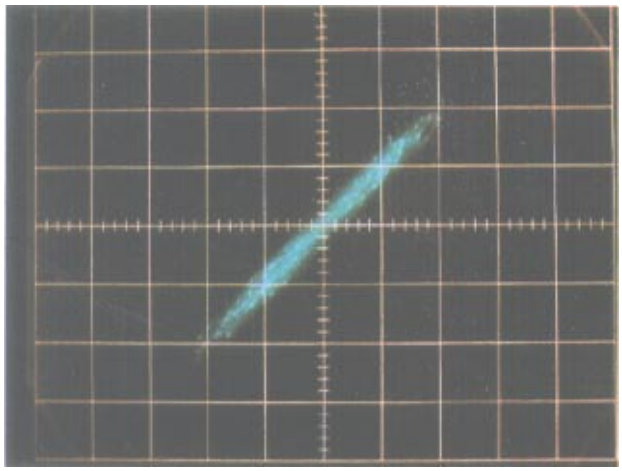

(b)

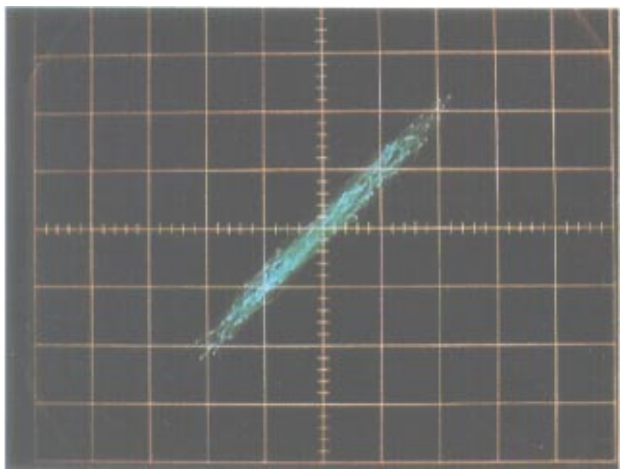

(c)

Fig. 9. Robustness of impulsive synchronization between Chua's oscillators to additive noise under the condition $T = 5.0 \times 10^{-6}$ s. Oscilloscope traces on the v_2–v_2' planes are shown. (a) Q/T is equal to 8%. (b) Q/T is equal to 50%. (c) Q/T is equal to 100%. This condition is equivalent to continuous synchronization.

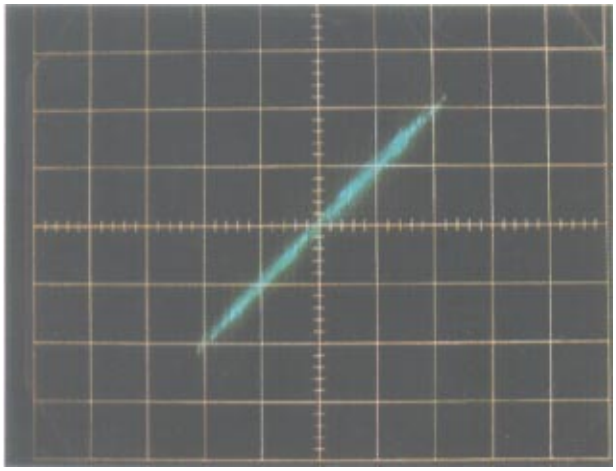

(a)

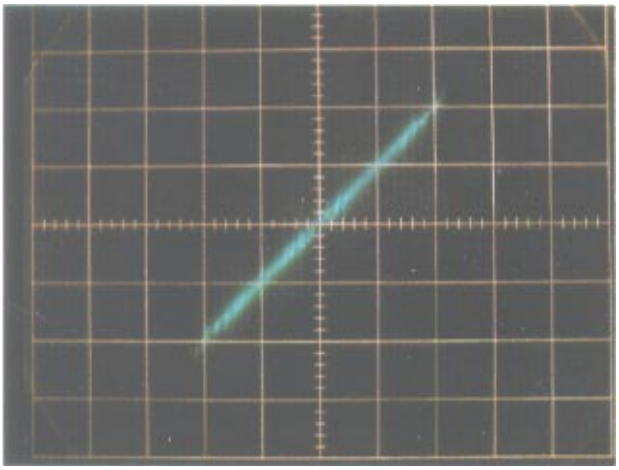

(b)

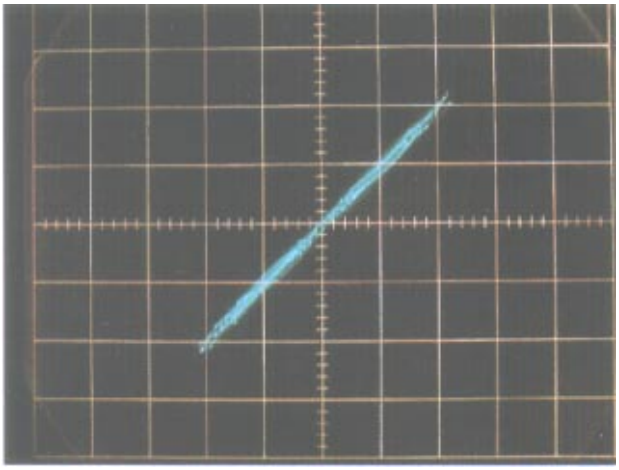

(c)

Fig. 10. Robustness of impulsive synchronization between Chua's oscillators to additive noise under the condition $T = 5.0 \times 10^{-6}$ s. Oscilloscope traces on the i–i' planes are shown. (a) Q/T is equal to 8%. (b) Q/T is equal to 50%. (c) Q/T is equal to 100%. This condition is equivalent to continuous synchronization.

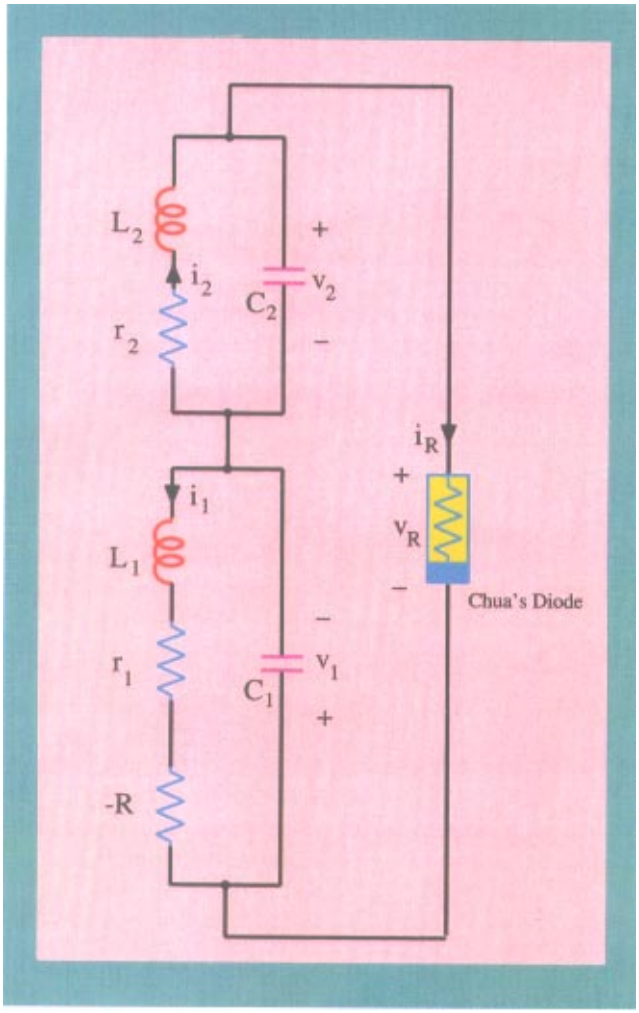

Fig. 11. Circuit diagram of the hyperchaotic circuit used in our experiments.

et al., 1986]. The state equation of this circuit is given by

$$C_1 \frac{dv_1}{dt} = g(v_2 - v_1) - i_1 \,, \tag{7}$$

$$C_2 \frac{dv_2}{dt} = -g(v_2 - v_1) - i_2 \,, \tag{8}$$

$$L_1 \frac{di_1}{dt} = v_1 - r_1 i_1 + R i_1 \,, \tag{9}$$

$$L_2 \frac{di_2}{dt} = v_2 - r_2 i_2 \,, \tag{10}$$

where $g(\cdot)$ is the v–i characteristic of Chua's diode, defined by

$$g(v_2 - v_1) = G_a (v_2 - v_1) + \frac{1}{2}(G_b - G_a) \times \left(|v_2 - v_1 - B_p| - |v_2 - v_1 + B_p| \right) , \tag{11}$$

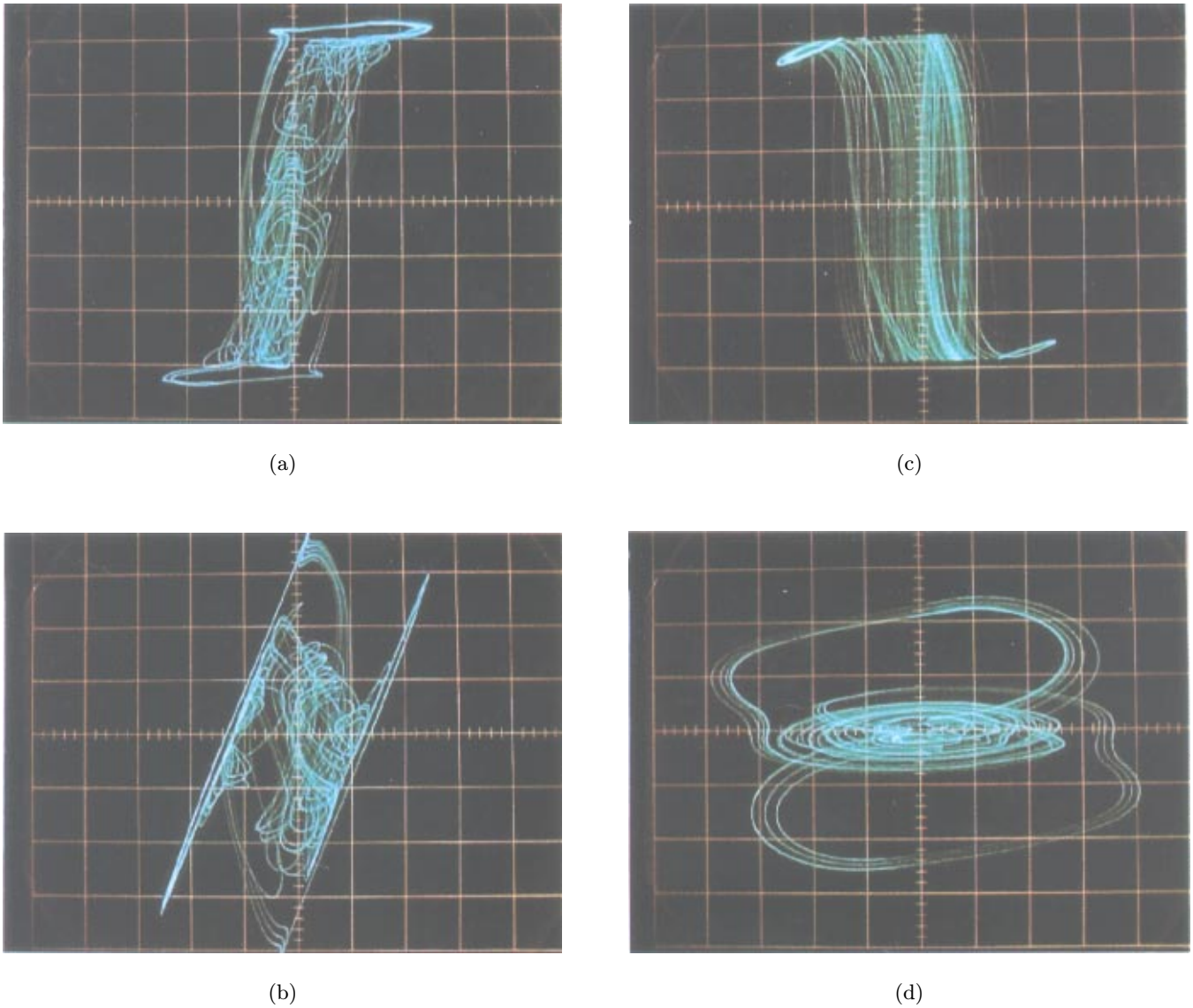

(a) (c)

(b) (d)

Fig. 12. Observed strange attractor from the hyperchaotic circuit used in our experiments. (a) Projection of the chaotic attractor onto the (v_1, $v_2 - v_1$)-plane. (b) Projection of the chaotic attractor onto the (v_1, v_2)-plane. (c) Projection of the chaotic attractor onto the (v_1, i_1)-plane. (d) Projection of the chaotic attractor onto the (v_2, i_2)-plane.

where B_p is the breakpoint voltage of Chua's diode. The parameters are chosen as follows:

$$C_1 = 102 \text{ nF}, \quad C_2 = 318 \text{ nF}, \quad L_1 = 29.9 \text{ mH}, \\ L_2 = 22.3 \text{ mH}, \quad R = 330\ \Omega, \tag{12}$$

$$r_1 = 71.2\ \Omega, \quad r_2 = 42.9\ \Omega, \quad G_a = 31.6 \text{ mS}, \\ G_b = -0.667 \text{ mS}, \quad B_p = 0.50 \text{ V}. \tag{13}$$

These parameters are different from the original parameters used in [Matsumoto *et al.*, 1986] because we have some difficulties in building a circuit with the same parameters. Different projections of the observed attractor for this hyperchaotic circuit are shown in Fig. 12.

The circuit diagram of impulsive synchronization of the two hyperchaotic circuits is shown in Fig. 13. The two voltage buffers send two signals v_2–v_1 and $-Ri_1$ to a switch controlled by two switching signals. Although samples from the two signals are sent to the driven circuit, we use a time-division scheme to transmit *both* impulse sequences through *only one* communication channel. In this case, each frame consists of three regions. The first two regions are synchronization regions consisting of driving impulses. The first region is used

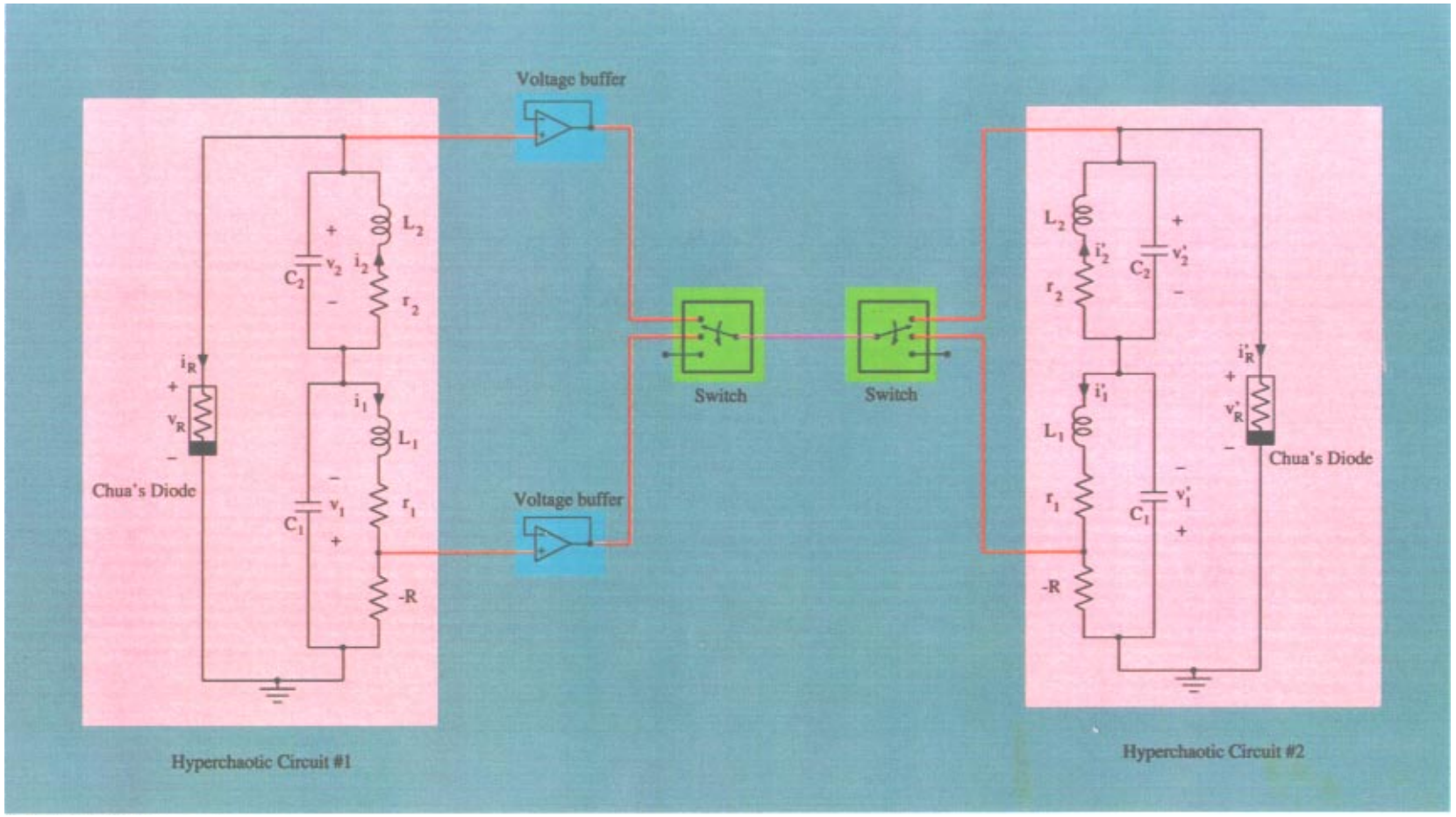

Fig. 13. Circuit diagram of impulsive synchronization between two hyperchaotic circuits.

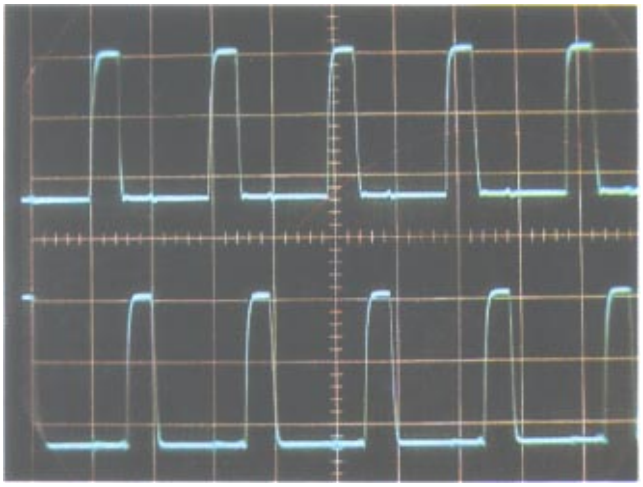

Fig. 14. Two switching signals are used to implement our time-division scheme for sending two impulse sequences through a single channel.

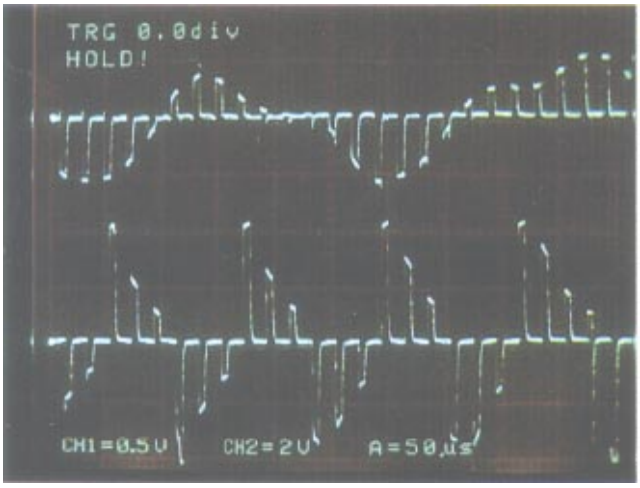

(a)

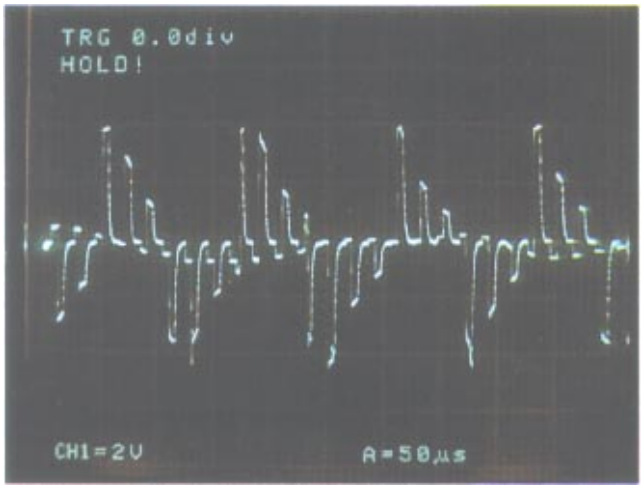

(b)

Fig. 15. Impulse sequences for impulsive synchronization of two hyperchaotic circuits. (a) Two impulse sequences shown separately. The upper trace is the impulse sequence sampled from the voltage v_2–v_1 across Chua's diode. The lower trace is the impulse sequence sampled from the voltage $-Ri$ across the negative resistor. (b) The transmitted impulse sequence through a single channel shared by the two impulse sequences shown in (a) under our time-division scheme.

to transmit synchronization impulses sampled from signal v_2–v_1, and the second region is used to transmit those sampled from signal $-Ri_1$. The third region can be used to transmit scrambled message signals. In the experiments presented in this section, we did not use the third region to transmit message signals. Figure 14 shows the two switching signals used to choose and set the timing of two kinds of synchronization impulses sampled from v_2–v_1 and $-Ri_1$. Observe that the time shift between the high voltage levels in these two switching signals correspond to the time-division scheme for sending both impulse sequences through a single channel. Figure 15(a) shows two synchronization impulse sequences sampled from v_2–v_1 and $-Ri_1$. Observe that the slight time shift between these two sequences corresponds to the two switching signals shown in Fig. 14. Figure 15(b) shows the impulse sequence transmitted through the single channel. Observe that these two kinds of synchronization impulses are transmitted over different time slots in each frame. Figures 16(a) and 16(b) show the tracings in the v_1–v_1' plane and v_2–v_2' plane for $Q/T = 0.26$ and $T = 4.0 \times 10^{-6}$ s, respectively. Observe that an almost-identical synchronization is achieved.

The experimental results of the relations between Q and T are summarized in Fig. 17. Figure 17(a) shows the relation between Q and T. Observe that the relationship is almost piecewise-linear. In Fig. 17(b), we enlarged the "almost linear" region shown in the black box in Fig. 17(a). Figure 17(c) shows the relation between Q and the impulse frequency F. Figure 17(d) shows the relation between Q/T and T. Correspondingly, we show the relation between Q/T and F in Fig. 17(e). The following conclusions can be drawn from our experimental observations.

(1) For 0.8×10^{-6} s $\leq T \leq 3.8 \times 10^{-6}$ s

The ratio Q/T falls from 47% to 26% as T increases. The available region $T - 2Q$ for transmitting scrambled signals increases gradually.

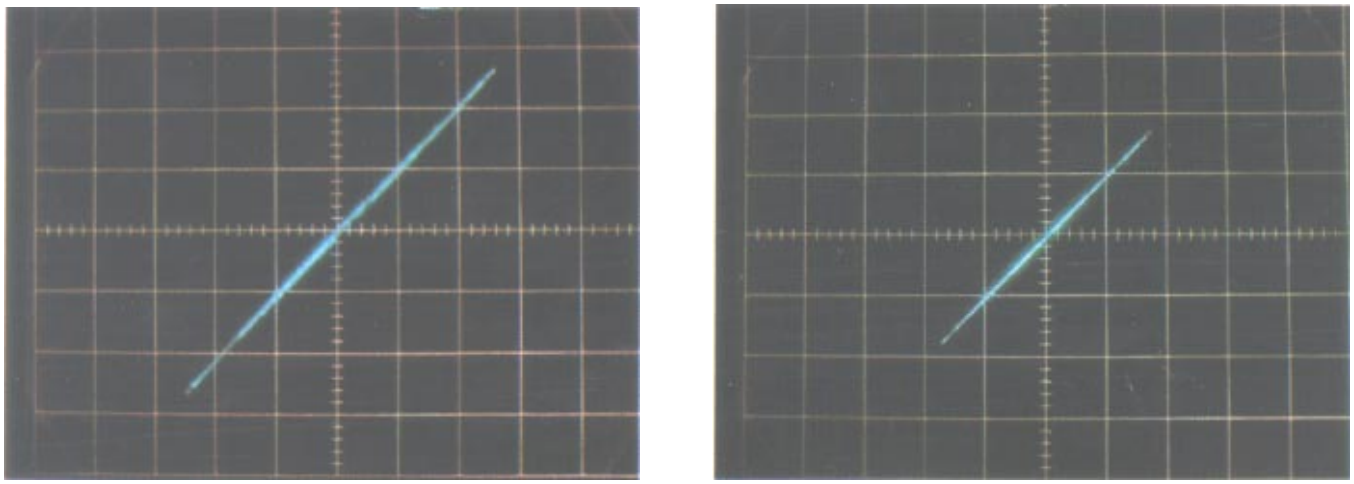

(a) (b)

Fig. 16. Impulsive synchronization between two hyperchaotic circuits under the conditions $Q/T = 0.26$ and $T = 4.0 \times 10^{-6}$ s. (a) Oscilloscope trace of v_1 versus v_1'. (b) Oscilloscope trace of v_2 versus v_2'.

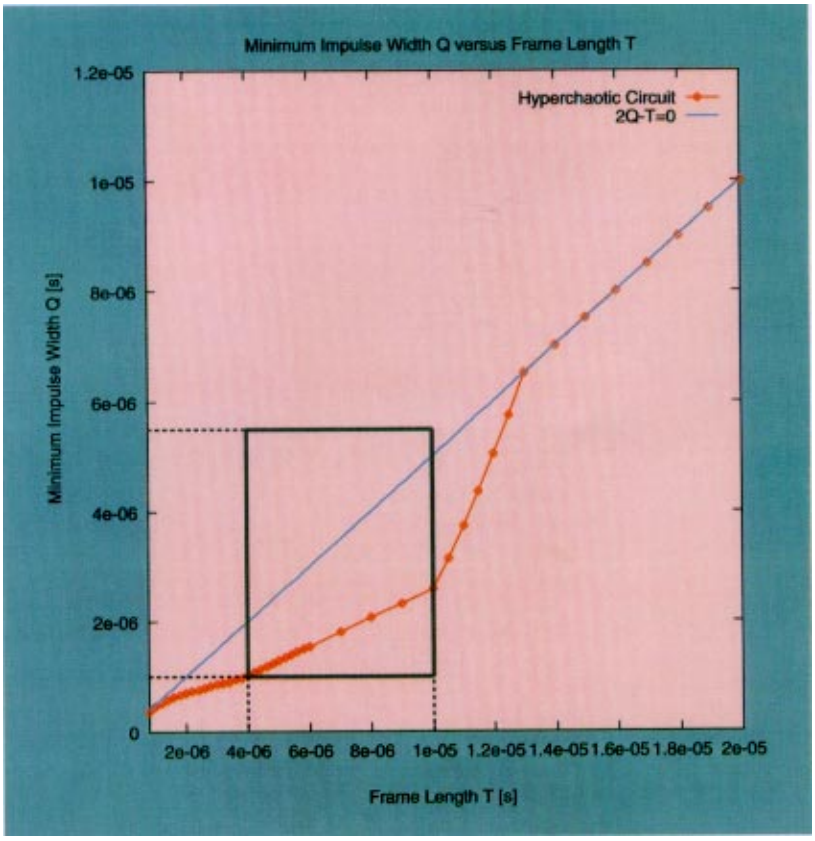

(a)

Fig. 17. The relationship between the minimum impulse width Q for achieving an almost-identical synchronization of two hyperchaotic circuits and the frame length T, or frequency of impulses $F = 1/T$. (a) Q versus T from 0 to 2×10^{-5} s. The upper straight line $Q = 1/2T$ is shown for comparison purpose. (b) Q versus T (over the range of 2×10^{-6} s $\leq T \leq 7 \times 10^{-5}$ s). (c) Q versus frequency F. (d) Ratio Q/T versus T. (e) Ratio Q/T versus frequency F.

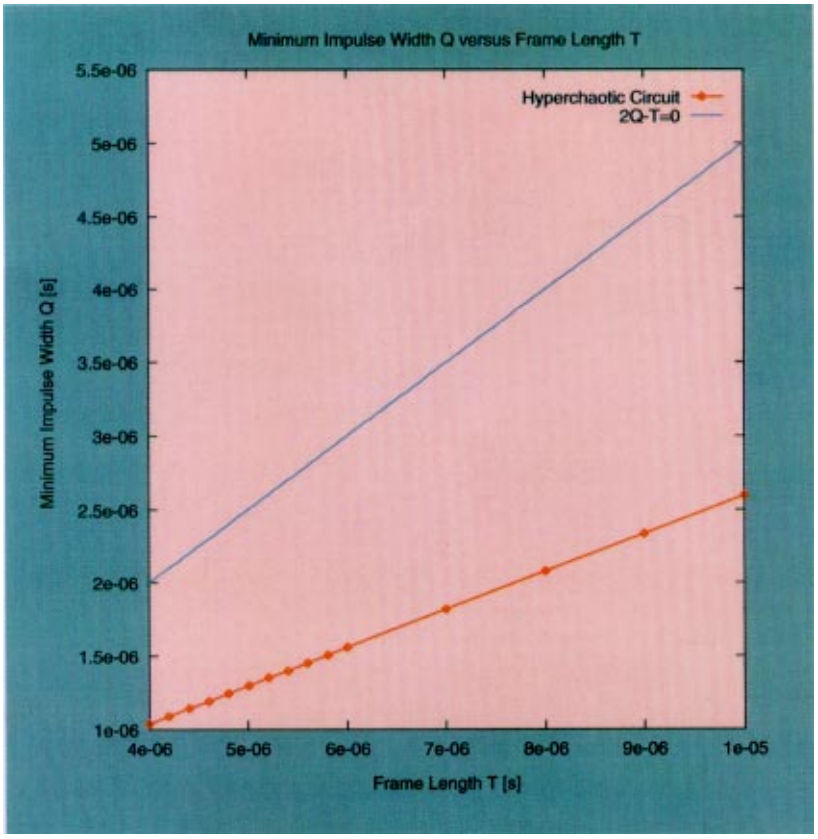

(b)

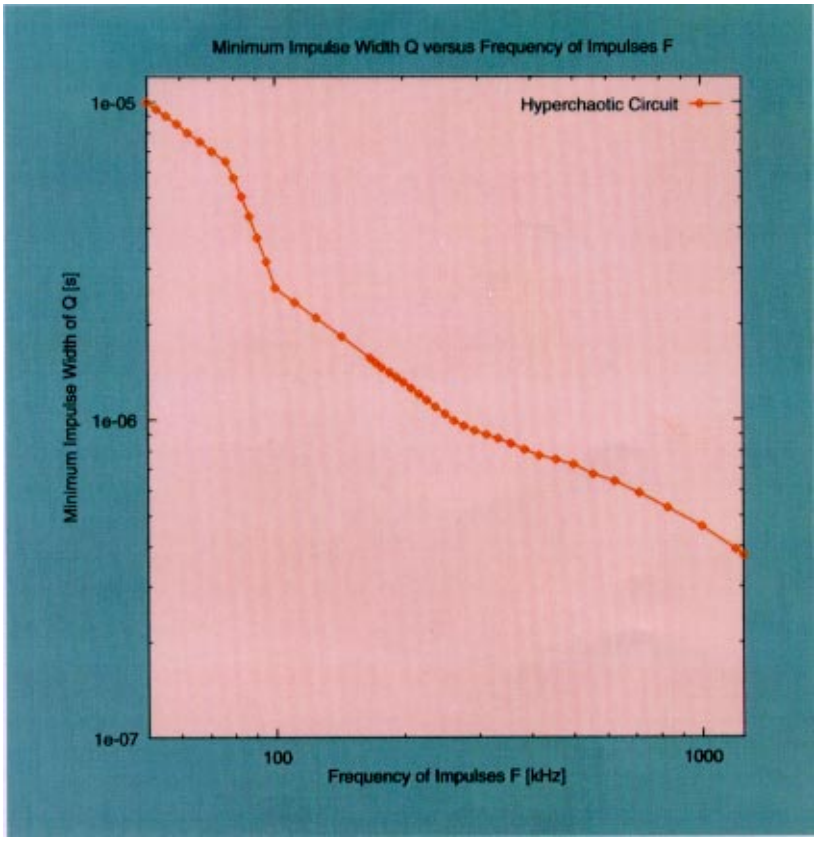

(c)

Fig. 17. (*Continued*)

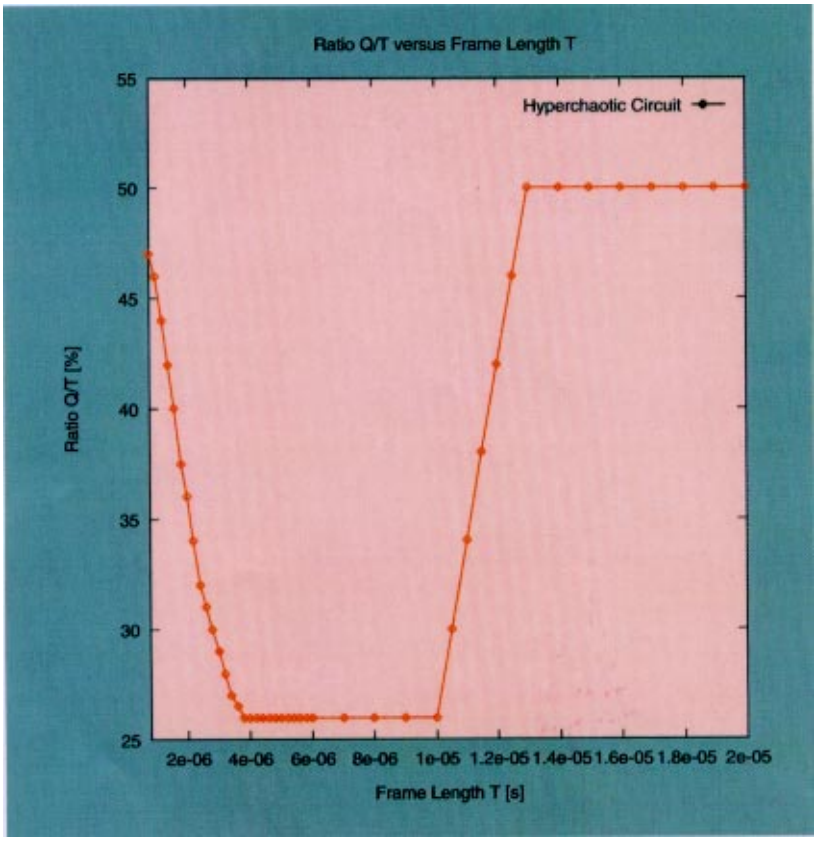

(d)

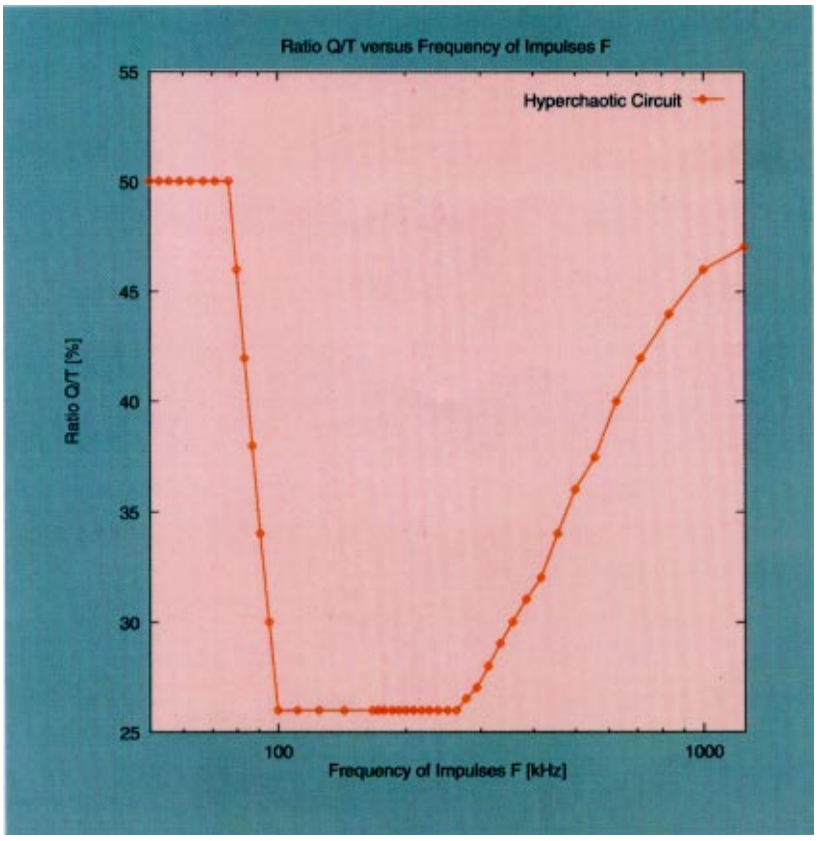

(e)

Fig. 17. (*Continued*)

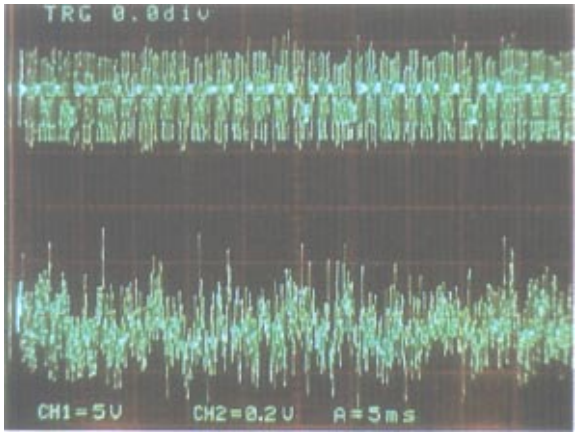

(a)

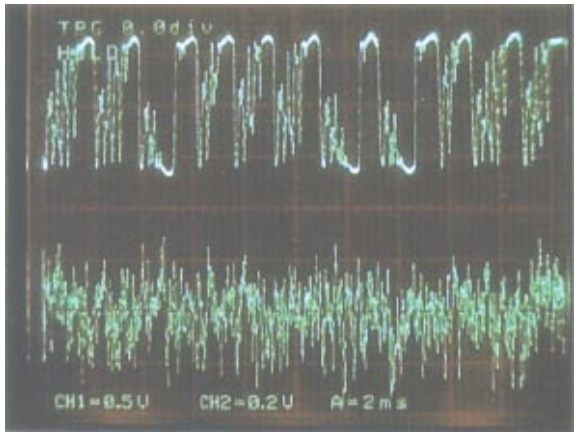

(b)

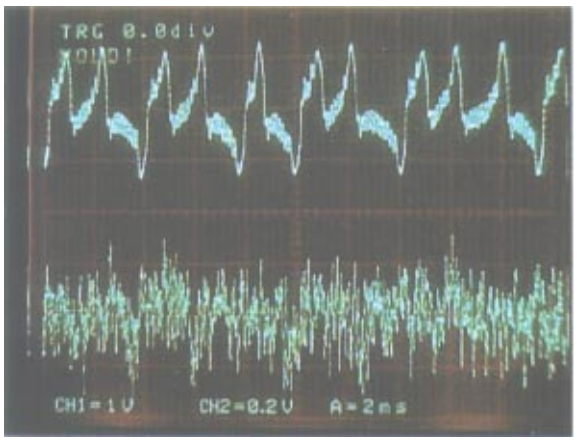

(c)

Fig. 18. Impulse sequence and additive noise. Horizontal scale is 2 ms/div. (a) The transmitted signal (upper trace) and the additive noise (lower trace). Vertical scales are 5.0 V/div for the upper trace and 0.2 V/div for the lower trace, respectively. (b) The signal v_2–v_1 (upper trace) and the additive noise (lower trace). Vertical scales are 0.5 V/div for the upper trace and 0.2 V/div for the lower trace, respectively. (c) The signal v_1 (upper trace) and the additive noise (lower trace). Vertical scales are 1.0 V/div for the upper trace and 0.2 V/div for the lower trace, respectively.

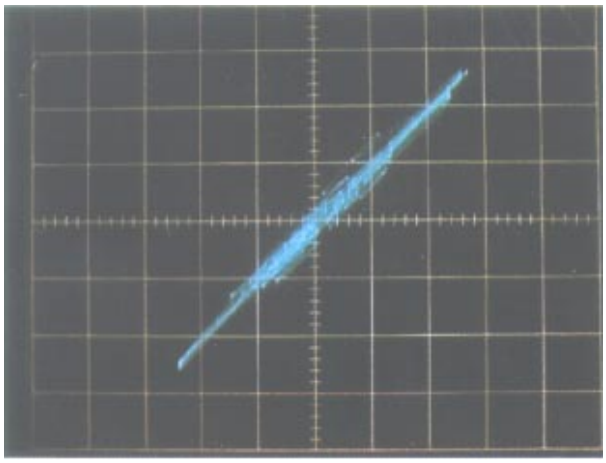

(a)

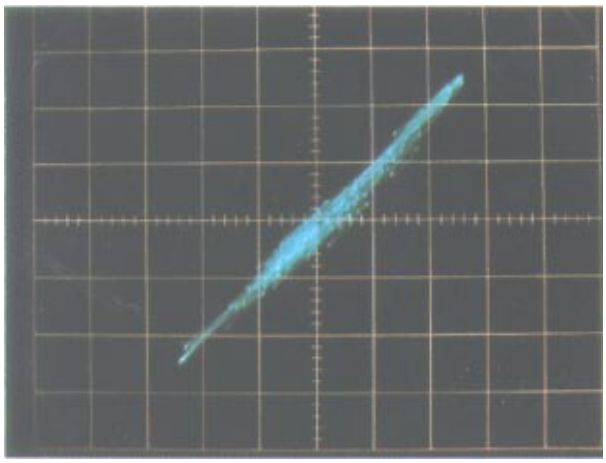

(b)

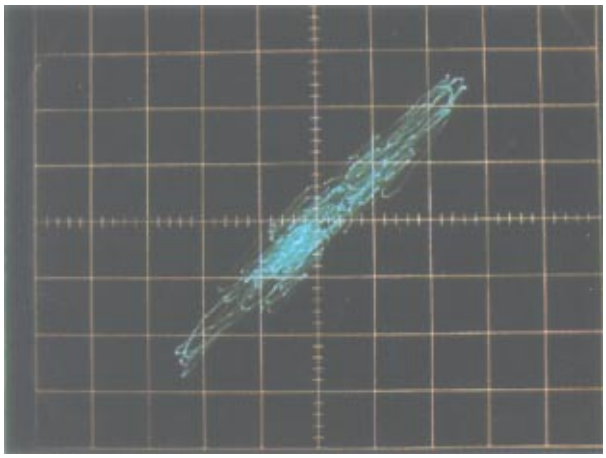

(c)

Fig. 19. Impulsive synchronization between two hyperchaotic circuits when the additive channel noise shown in Fig. 18 is added with $T = 4.0 \times 10^{-6}$s. (a) Oscilloscope trace of v_1 versus v_1' with $Q/T = 0.26$. (b) Oscilloscope trace of v_1 versus v_1' with $Q/T = 0.40$. (c) Oscilloscope trace of v_1 versus v_1' with $Q/T = 1.0$; namely, continuous synchronization.

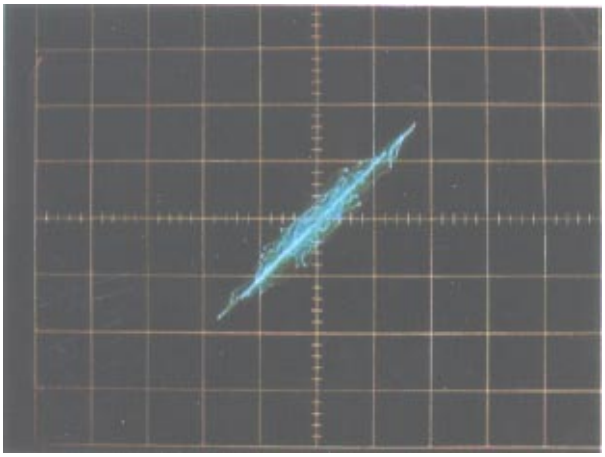

(a)

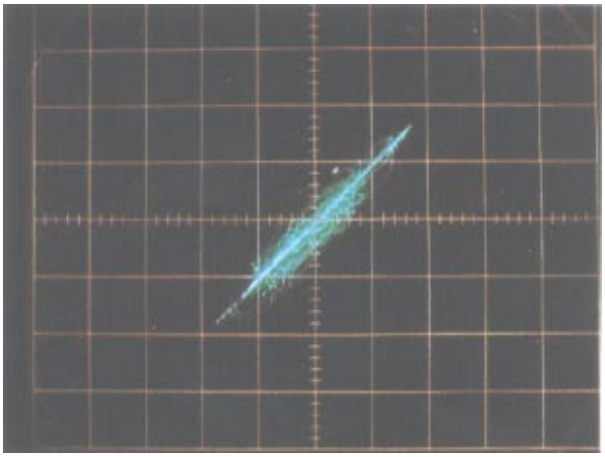

(b)

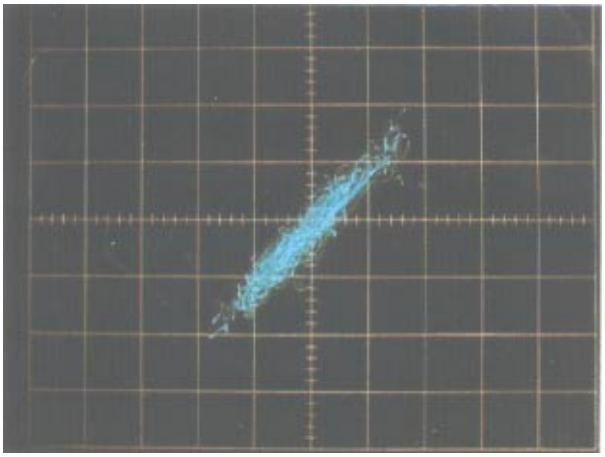

(c)

Fig. 20. Impulsive synchronization between two hyperchaotic circuits when the additive channel noise shown in Fig. 18 is added with $T = 4.0 \times 10^{-6}$ s. (a) Oscilloscope trace of v_2 versus v_2' with $Q/T = 0.26$. (b) Oscilloscope trace of v_2 versus v_2' with $Q/T = 0.40$. (c) Oscilloscope trace of v_1 versus v_1' with $Q/T = 1.0$; namely, continuous synchronization.

(2) For 3.8×10^{-6} s $\leq T \leq 1.3 \times 10^{-5}$ s

The ratio Q/T is equal to 26%. In this case, an almost-identical synchronization requires at least 52% ($= 2Q/T = 26\% \times 2$) of the frame length for transmitting synchronization impulses. In this case, 48% of the frame length is available for transmitting message signals. In this case, Q increases in proportion to T.

(3) For 1.0×10^{-5} s $\leq T \leq 1.3 \times 10^{-5}$ s

The ratio Q/T rises from 26% to 50% as T increases. The available time slot for transmitting information signals decreases.

(4) For 1.3×10^{-5} s $\leq T \leq 2.0 \times 10^{-5}$ s

An almost-identical synchronization requires 100% ($= 50\% \times 2$) of the frame length for transmitting synchronization impulses. No time slot is available for transmitting information signals.

We then examine the robustness of the impulsive synchronization to small additive noise. Figure 18(a) shows the transmitted impulse sequence and the additive noise. To compare the amplitudes of impulses and noise, Fig. 18(b) shows the signal v_2–v_1 and the additive noise. Figure 18(c) shows the signal v_1 and the additive noise.

The experimental results are shown in Figs. 19 and 20 with $T = 4.0 \times 10^{-6}$ s. Figures 19(a)–19(c) show the oscilloscope traces on the v_1–v_1' planes with $Q/T = 26\%$, 40% and 100%, respectively. Figure 20(a)–20(c) show the oscilloscope traces on the v_2–v_2' planes with $Q/T = 26\%$, 40% and 100%, respectively. There is no observable difference between impulsive synchronization and continuous synchronization because in Figs. 19 and 20 the thickness of the 45-degree lines for impulsive synchronization and for continuous synchronization are almost the same. The above observations show that impulsive synchronization of the hyperchaotic circuit in Fig. 11 is robust to small additive noise.

3. Spread Spectrum Communication Systems

In chaotic spread spectrum communication systems, there are different ways to modulate the message signal $s(t)$ with a chaotic spreading carrier $c(t)$. For example, one can multiply $c(t)$ with $s(t)$ (direct sequence modulation [Yang & Chua, 1997a,

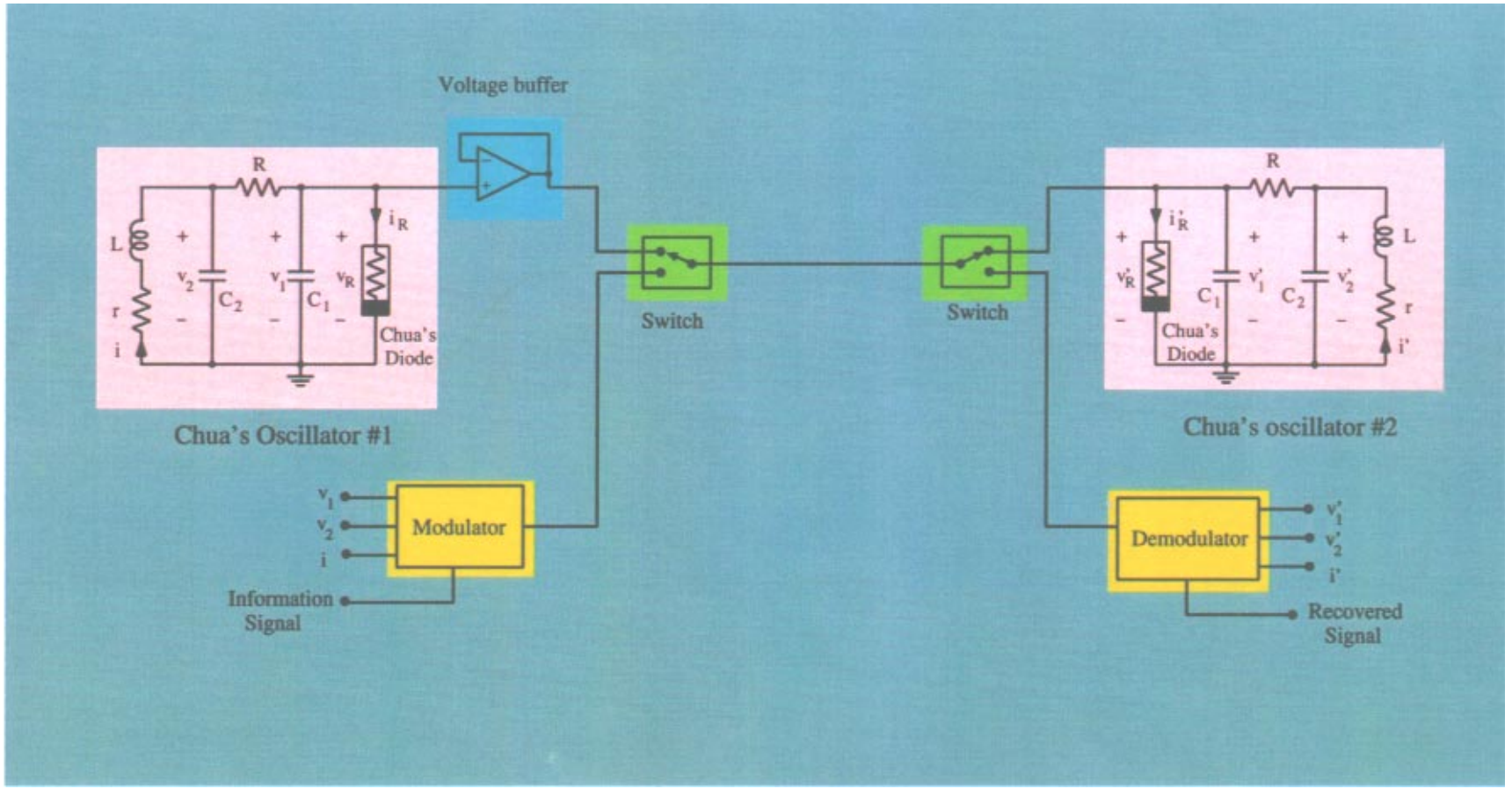

(a)

Fig. 21. Circuit diagrams of chaotic spread spectrum communication systems used in our experiments when additive and DS modulations are used. (a) When the Chua's oscillators are used to generate the chaotic spreading carriers. (b) When the hyperchaotic circuits are used to generate the chaotic spreading carriers.

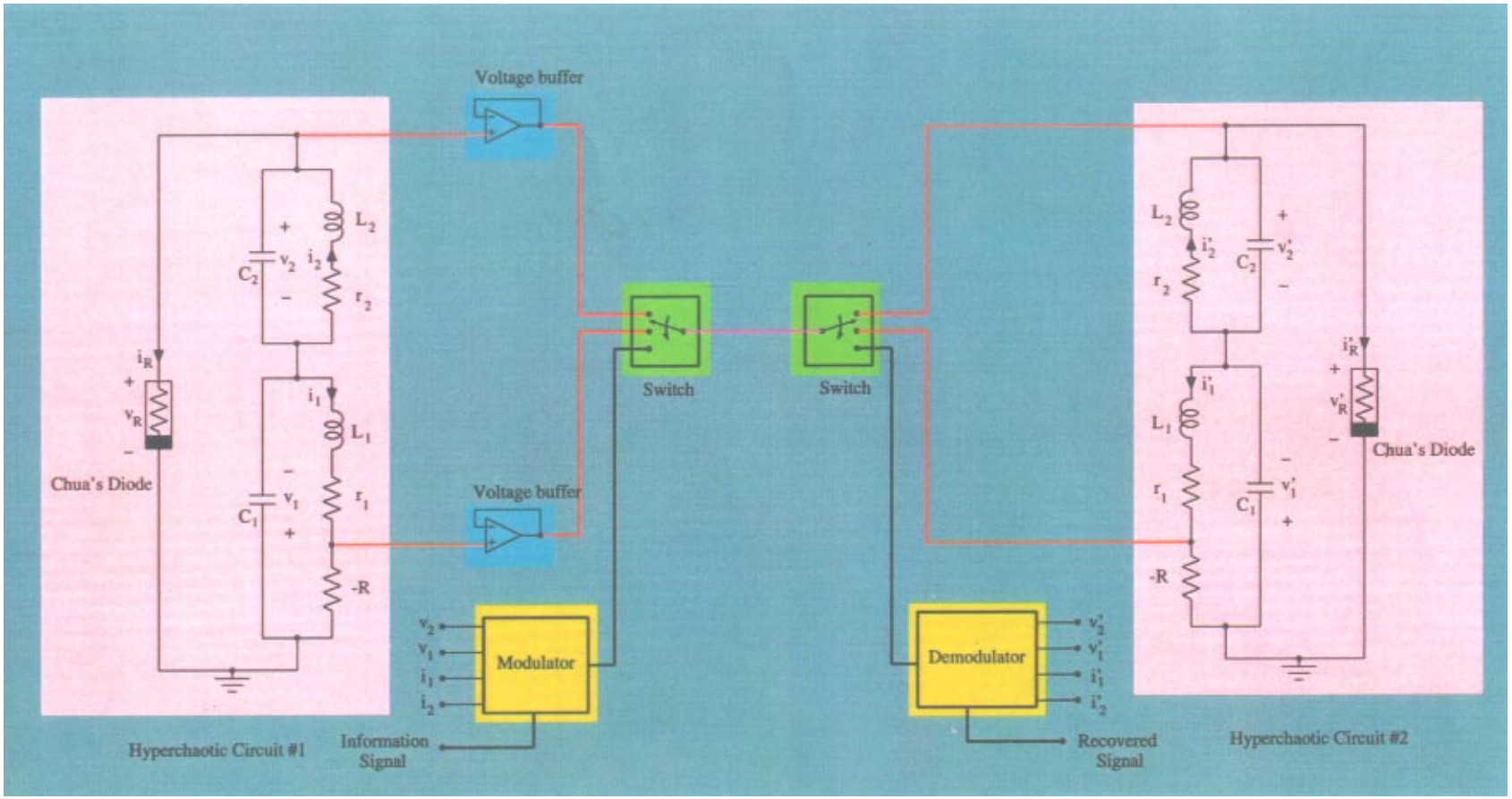

(b)

Fig. 21. (*Continued*)

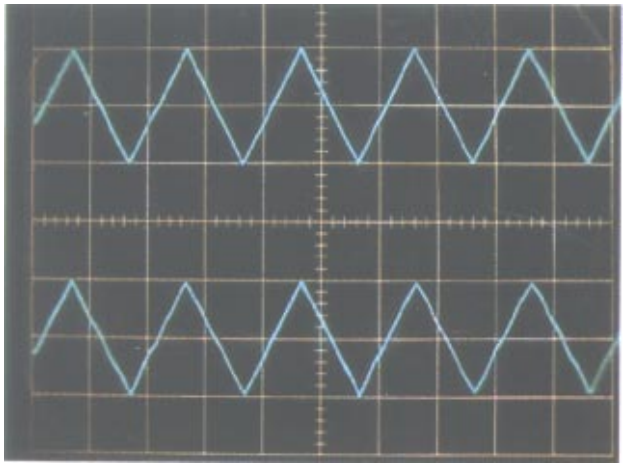

(a)

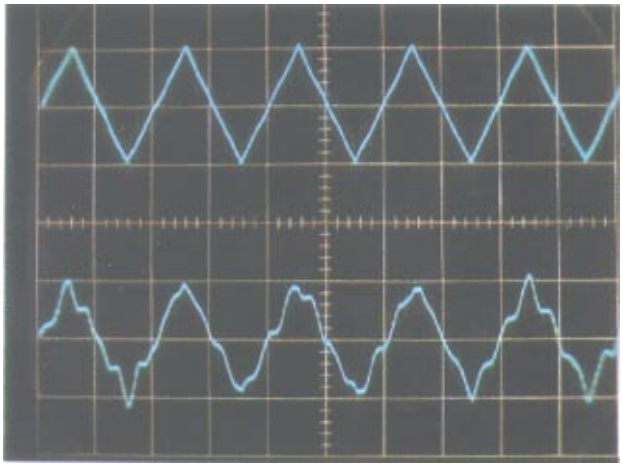

(d)

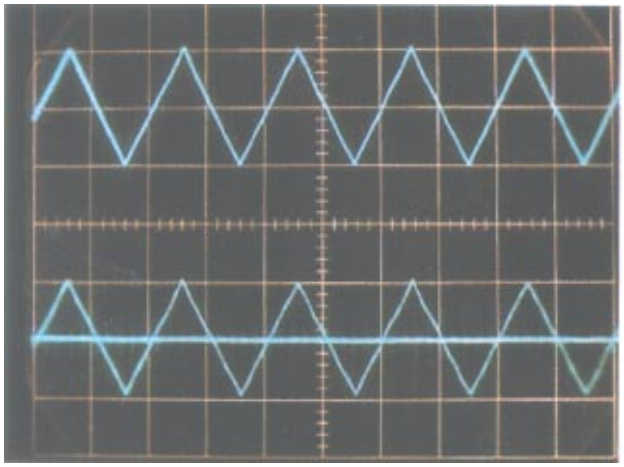

(b)

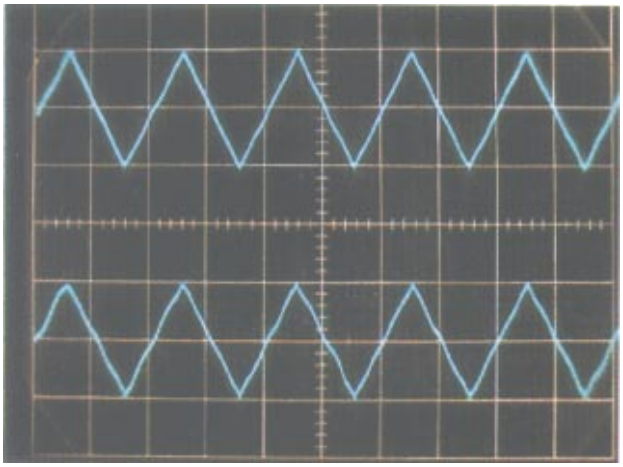

(e)

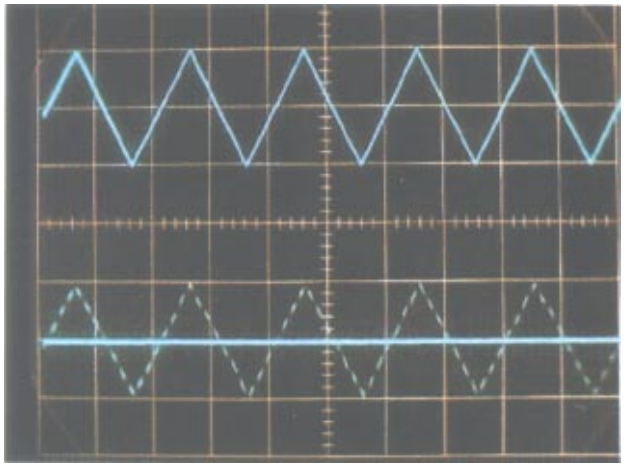

(c)

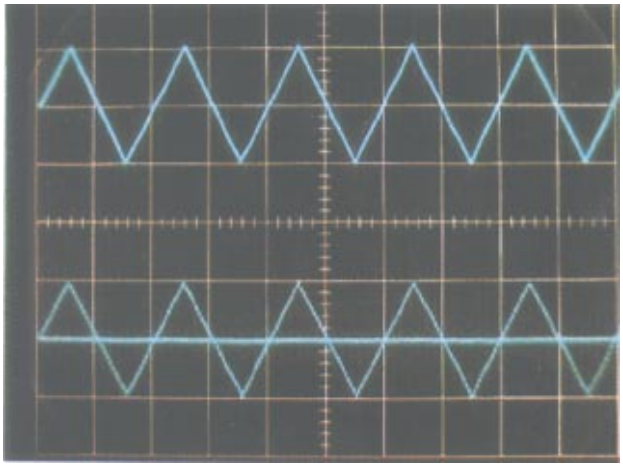

(f)

Fig. 22. Message signals and recovered message signals when the systems in Fig. 21(a) is used with additive modulation. Message signals are shown in upper traces and the recovered message signals are shown in lower traces. (a) $Q/T = 10\%$ and $T = 2.0 \times 10^{-5}$ s. (b) $Q/T = 50\%$ and $T = 2.0 \times 10^{-5}$ s. (c) $Q/T = 80\%$ and $T = 2.0 \times 10^{-5}$ s. (d) $Q/T = 8\%$ and $T = 8.0 \times 10^{-6}$ s. (e) $Q/T = 18\%$ and $T = 8.0 \times 10^{-6}$ s. (f) $Q/T = 50\%$ and $T = 8.0 \times 10^{-6}$ s.

1998a, 1998b; Itoh, 1999]). One can also add $s(t)$ to $c(t)$ (chaotic masking [Kocarev *et al.*, 1992]).

For relatively low security situations, we can easily implement the chaotic masking scheme by using impulsive synchronization. The synchronization region Q of each frame consists of synchronization impulses while the rest of the frame consists of the masked signal $p(t) = s(t) + c(t)$. The recovery of the message signal is performed by subtracting $\tilde{c}(t)$ from $p(t)$ within the region $T - Q$ (here, $\tilde{c}(t)$ is the chaotic carrier recovered using impulsive synchronization at the receiver end). Therefore, the recovering process is a little simpler than that proposed in [Kocarev *et al.*, 1992]. Similarly, the direct sequence (DS) modulation can be easily implemented by impulsive synchronization.

In the spread spectrum communication systems based on impulsive synchronization presented in this section, within each frame of T seconds, the message signal takes only $T - Q$ seconds. Since Q is not small with respect to T, the recovered signal $r(t)$ is periodically sampled for every T seconds. Thus, for a reliable recovery the message signal $s(t)$ should be bandlimited to a frequency range below $1/2T$ in accordance with the sampling theorem.

The block diagram of the chaotic spread spectrum communication systems based on impulsive synchronization is shown in Fig. 21. Figure 21(a) shows the block diagram based on Chua's oscillators. The modulator at the transmitter end will scramble the message signal with the chaotic masks by using either addition or multiplication. The switch is between v_1 and the modulated message signal. Correspondingly, Fig. 21(b) shows the block diagram based on hyperchaotic circuits.

The experimental results with Chua's oscillators and additive modulation are shown in Fig. 22. The message signal is a triangular waveform. Figure 22(a) shows the message signal and the recovered message signal under the conditions $Q/T = 10\%$ and $T = 2.0 \times 10^{-5}$ s. Figure 22(b) shows the message signal and the recovered message signal under the conditions $Q/T = 50\%$ and $T = 2.0 \times 10^{-5}$ s. Figure 22(c) shows the message signal and the recovered message signal under the conditions $Q/T = 80\%$ and $T = 2.0 \times 10^{-5}$ s. Observe from Figs. 22(a)–22(c) that the recovered signals have very little distortions. Figure 22(d) shows the message signal and the recovered message signal under the conditions $Q/T = 8\%$ and $T = 8.0 \times 10^{-6}$ s. Significant distortions in the recovered message signal can now be observed. Figure 22(e) shows the message signal and the recovered message signal under the conditions $Q/T = 18\%$ and $T = 8.0 \times 10^{-6}$ s. Figure 22(f) shows the message signal and the recovered message signal under the conditions $Q/T = 50\%$ and $T = 8.0 \times 10^{-6}$ s. Observe from Figs. 22(e) and 22(f) that the recovered signals have very little distortions.

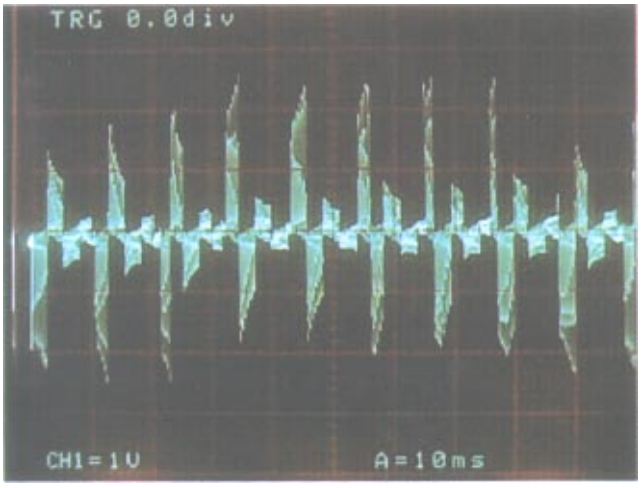

(a)

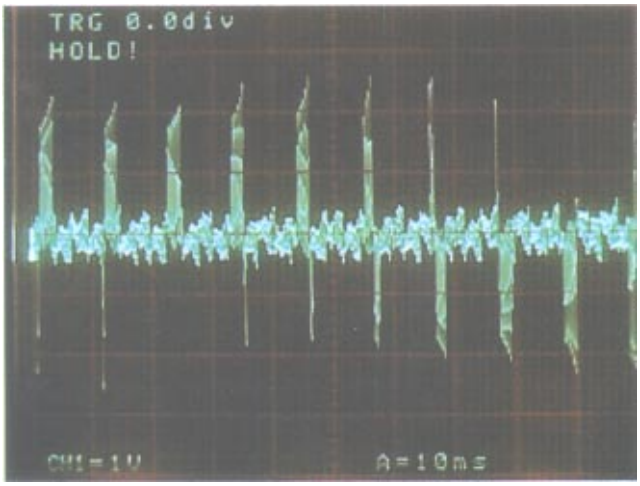

(b)

Fig. 23. The transmitted signals with or without modulated message signals under the conditions $Q/T = 10\%$ and $T = 2.0 \times 10^{-5}$ s. The chaotic systems are Chua's oscillators. (a) Transmitted signal without the modulated message signal. (b) Transmitted signal with the modulated message signal when additive modulation is used.

To show what the transmitted signal in the channel looks like, in Fig. 23(a) the mixture of the impulse sequence and the chaotic carrier $c(t)$ is shown. Figure 23(b) shows the mixture of the

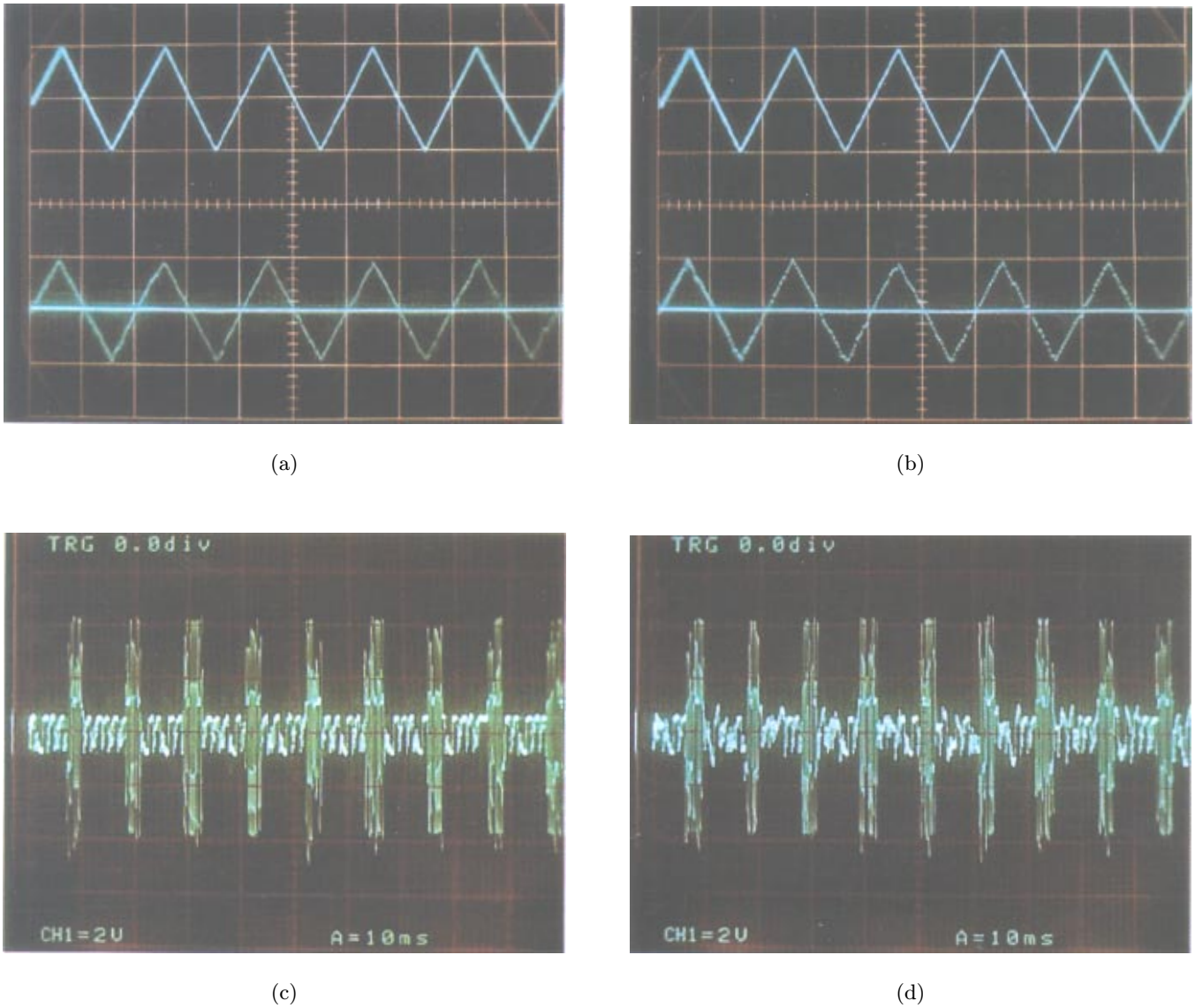

(a) (b)

(c) (d)

Fig. 24. Different kinds of signals observed in experiments when hyperchaotic circuits and additive modulation are used. (a) Message signal (the upper trace) and recovered message signal (the lower trace). $Q/T = 26\%$ and $T = 5.0 \times 10^{-6}$ s. (b) Message signal (the upper trace) and recovered message signal (the lower trace). $Q/T = 26\%$ and $T = 8.0 \times 10^{-6}$ s. (c) Transmitted signal without the modulated message signal. (d) Transmitted signal with the modulated message signal.

impulse sequence and the modulated message signal $c(t) + s(t)$.

Our experimental results on the hyperchaotic circuits with additive modulation are shown in Fig. 24. The message signal is also a triangular waveform. Figure 24(a) shows the message signal and the recovered message signal under the conditions $Q/T = 26\%$ and $T = 5.0 \times 10^{-6}$ s. Figure 24(b) shows the message signal and the recovered message signal under the conditions $Q/T = 26\%$ and $T = 8.0 \times 10^{-6}$ s. Observe that there exists almost no distortions in the recovered signals. To show what the transmitted signal in the channel looks like, in Fig. 24(c) the mixture of the impulse sequence and the chaotic carrier $c(t)$ is shown. Figure 24(d) shows the mixture of the impulse sequence and the modulated message signal $c(t) + s(t)$.

In the DS modulation, the message signal is multiplied by the chaotic spreading carrier at the transmitter and the transmitted signal is divided by the recovered chaotic spreading carrier at the receiver end. In our experiments, we use AD533 IC chips as multipliers and dividers. In the AD533

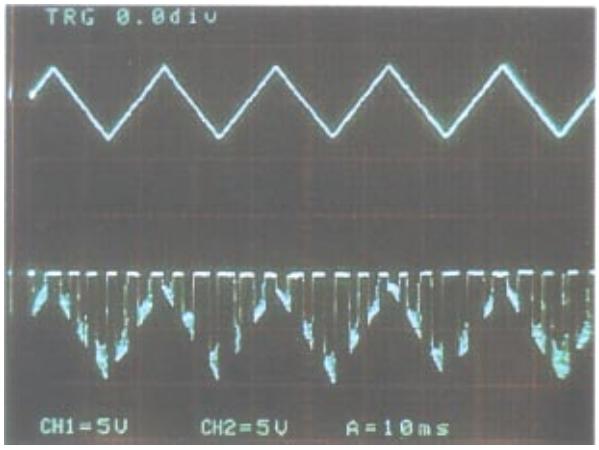

(a)

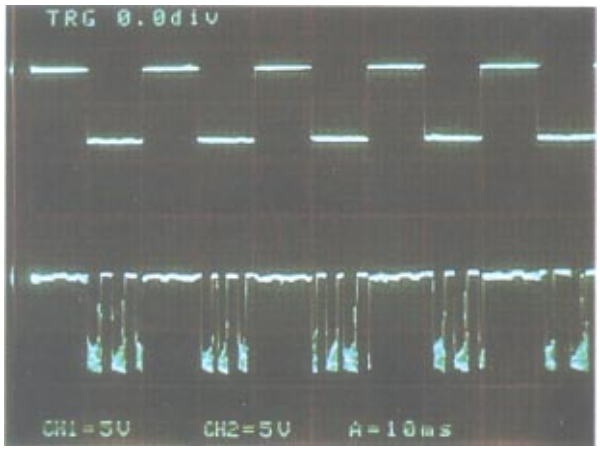

(b)

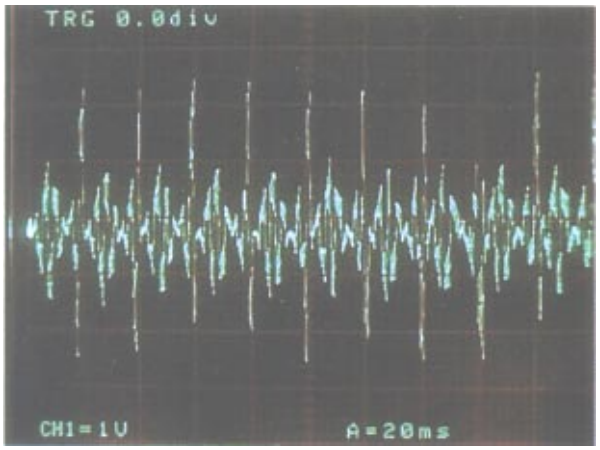

(c)

Fig. 25. Experimental results when DS modulation and Chua's oscillators are used. v_1 is chosen as the chaotic spreading carrier. $Q/T = 10\%$ and $T = 2.0 \times 10^{-5}$ s. (a) The triangular message signal $s(t)$ (the upper trace) and the recovered message signal $r(t)$ (the lower trace). (b) The binary message signal $s(t)$ (the upper trace) and the recovered message signal $r(t)$ (the lower trace). (c) Transmitted signal.

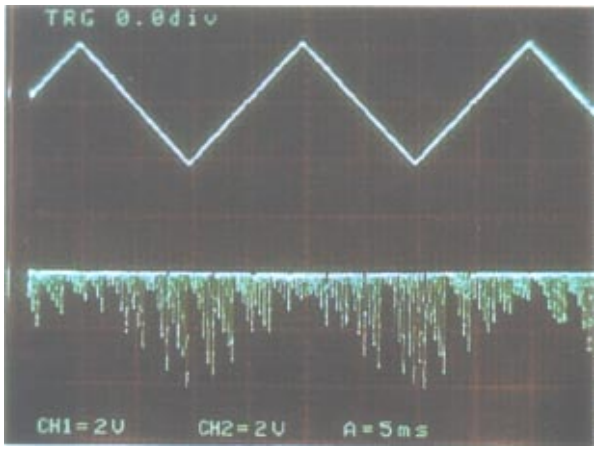

(a)

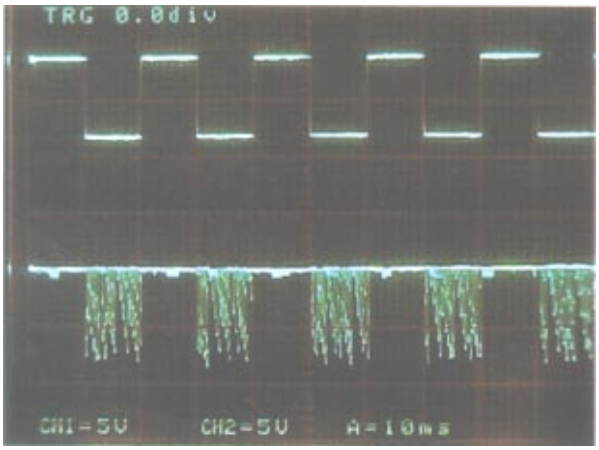

(b)

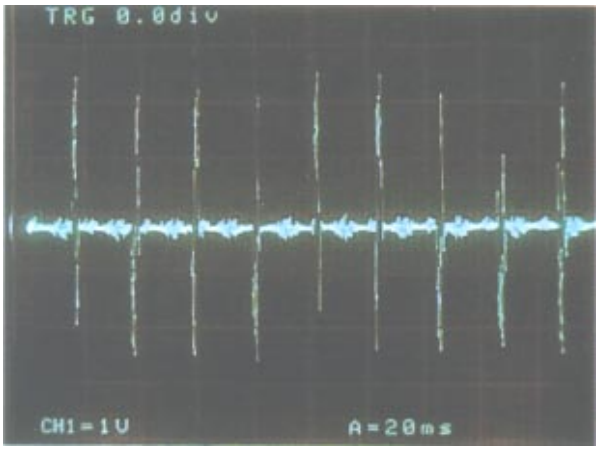

(c)

Fig. 26. Experimental results when DS modulation and Chua's oscillators are used. v_2 is chosen as the chaotic spreading carrier. $Q/T = 10\%$ and $T = 2.0 \times 10^{-5}$ s. (a) The triangular message signal $s(t)$ (the upper trace) and the recovered message signal $r(t)$ (the lower trace). (b) The binary message signal $s(t)$ (the upper trace) and the recovered message signal $r(t)$ (the lower trace). (c) Transmitted signal.

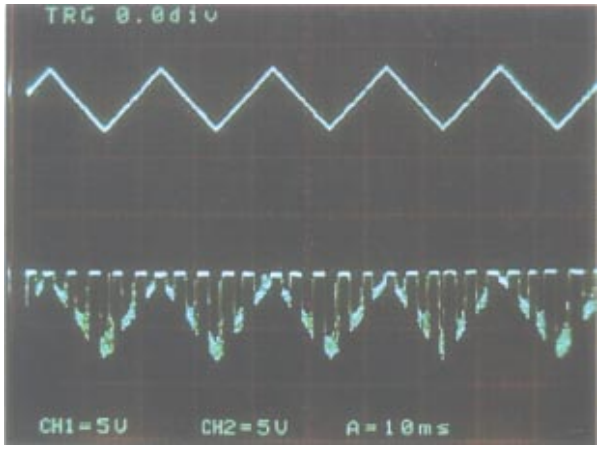

(a)

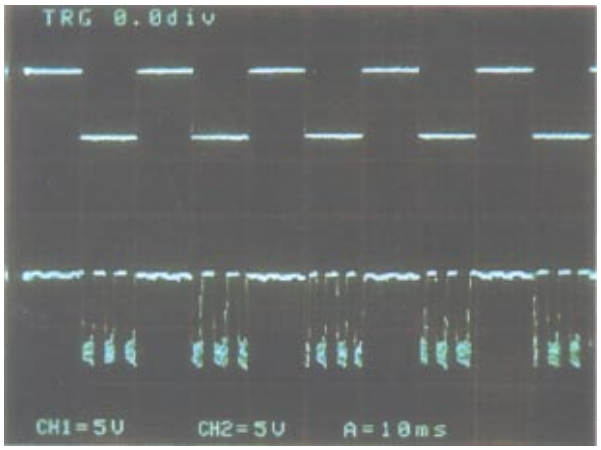

(b)

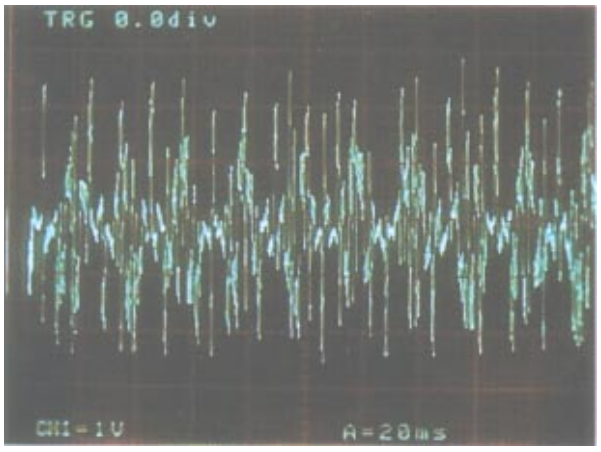

(c)

Fig. 27. Experimental results when DS modulation and Chua's oscillators are used. Here, v_1 is chosen as the chaotic spreading carrier. $Q/T = 8\%$ and $T = 8.0 \times 10^{-6}$ s. (a) The triangular message signal $s(t)$ (the upper trace) and the recovered message signal $r(t)$ (the lower trace). (b) The binary message signal $s(t)$ (the upper trace) and the recovered message signal $r(t)$ (the lower trace). (c) Transmitted signal.

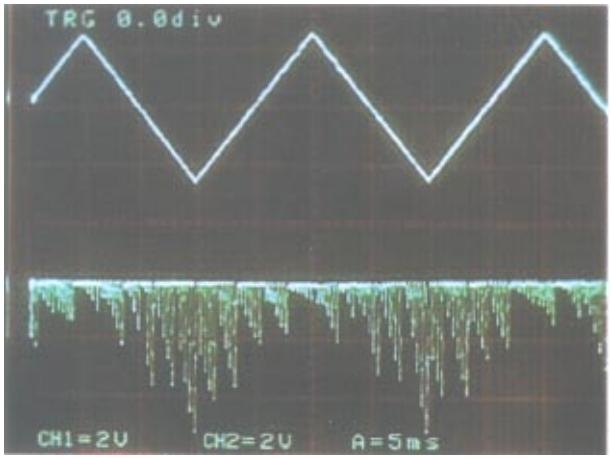

(a)

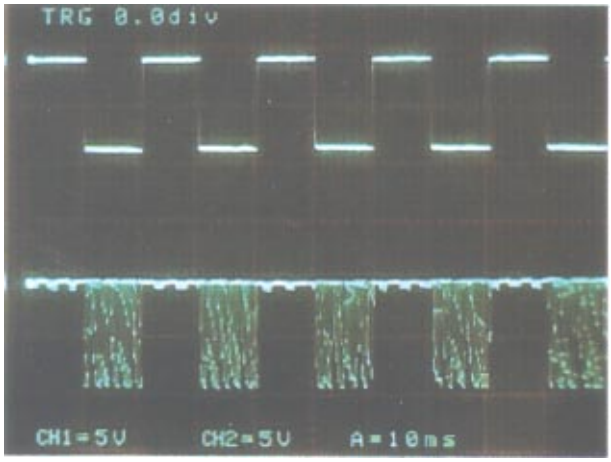

(b)

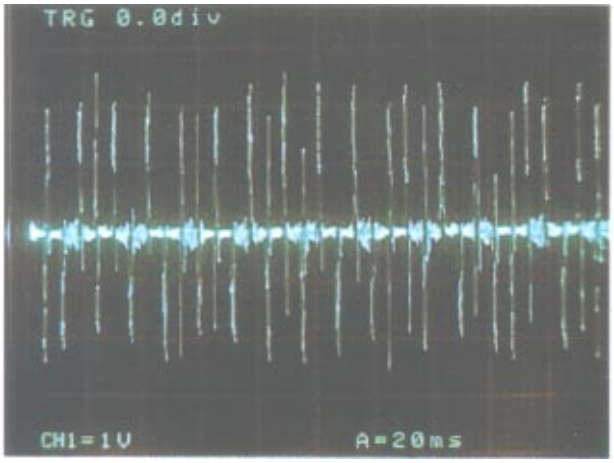

(c)

Fig. 28. Experimental results when DS modulation and Chua's oscillators are used. Here, v_2 is chosen as the chaotic spreading carrier. $Q/T = 8\%$ and $T = 8.0 \times 10^{-6}$ s. (a) The triangular message signal $s(t)$ (the upper trace) and the recovered message signal $r(t)$ (the lower trace). (b) The binary message signal $s(t)$ (the upper trace) and the recovered message signal $r(t)$ (the lower trace). (c) Transmitted signal.

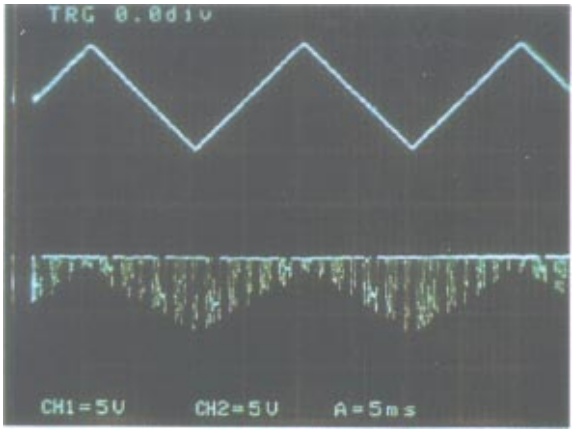

(a)

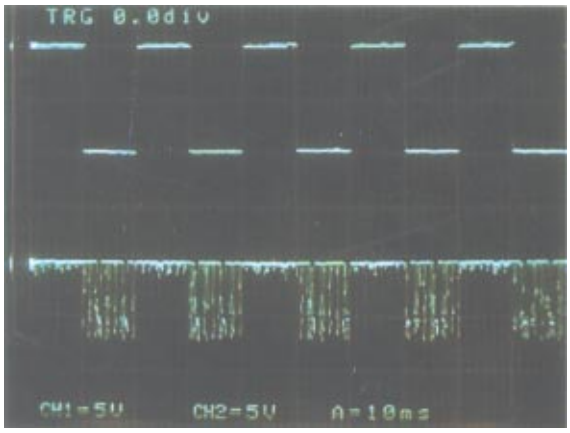

(b)

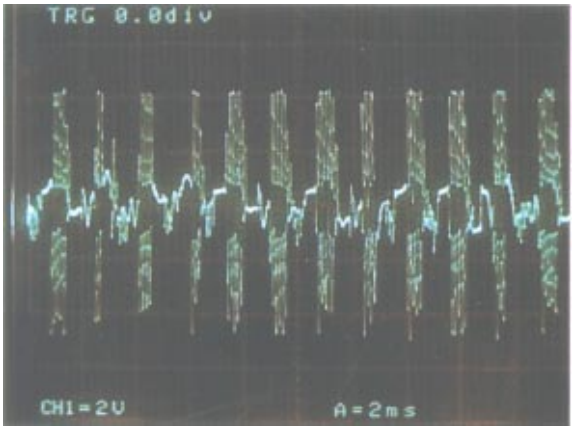

(c)

Fig. 29. Experimental results when DS modulation and hyperchaotic circuits are used. Here, v_2–v_1 is chosen as the chaotic spreading carrier. $Q/T = 34\%$ and $T = 2.5 \times 10^{-6}$ s. (a) The triangular message signal $s(t)$ (the upper trace) and the recovered message signal $r(t)$ (the lower trace). (b) The binary message signal $s(t)$ (the upper trace) and the recovered message signal $r(t)$ (the lower trace). (c) Transmitted signal.

chip, the division operations are not performed in the negative regions of the input signals, thereby giving rise to interruptions in the recovering process. Furthermore, the recovered signals are saturated in the negative regions. If AD532 chips are used instead, then the division is performed well in the negative regions and better results can be expected.

The experimental results for the DS modulation when Chua's oscillators are used are shown in Figs. 25–28.

Figure 25 shows the results when the message signal $s(t)$ is modulated by $v_1(t)$; namely, the modulated message signal is $v_1(t)s(t)$. Conditions are given by: $Q/T = 10\%$ and $T = 2.0 \times 10^{-5}$ s. Figure 25(a) shows the triangular message signal and the recovered message signal. Figure 25(b) shows the binary message signal and the recovered message signal. Observe that whenever the recovered chaotic carrier $\tilde{v}_1(t)$ is in the negative region, the recovered result jumps to a saturated value. But the message signal is recovered when $\tilde{v}_1(t)$ is positive. Figure 25(c) shows the transmitted signal, which consists of both synchronization impulses and the modulated message signal.

Figure 26 shows the results when the message signal $s(t)$ is modulated by $v_2(t)$; namely, the modulated message signal is $v_2(t)s_1(t)$. Conditions are given by: $Q/T = 10\%$ and $T = 2.0 \times 10^{-5}$ s. Figure 26(a) shows the triangular message signal and the recovered message signal. Figure 26(b) shows the binary message signal and the recovered message signal. Since the recovered carrier $\tilde{v}_2(t)$ switches between positive and negative regions at a rather high frequency, the recovered signals are modulated by short impulses. By using low-pass filters, we can easily improve the recovered message signals. Figure 26(c) shows the transmitted signal, which consists of both synchronization impulses and the modulated message signal.

Figure 27 shows the results when the message signal $s(t)$ is modulated by $v_1(t)$ under the conditions $Q/T = 8\%$ and $T = 8.0 \times 10^{-6}$ s. Figure 27(a) shows the triangular message signal and the recovered message signal. Figure 27(b) shows the binary message signal and the recovered message signal. Figure 27(c) shows the transmitted signal, which consists of both synchronization impulses and the modulated message signal.

Figure 28 shows the results when the message signal $s(t)$ is modulated by $v_2(t)$ under the conditions $Q/T = 8\%$ and $T = 8.0 \times 10^{-6}$ s. Figure 27(a)

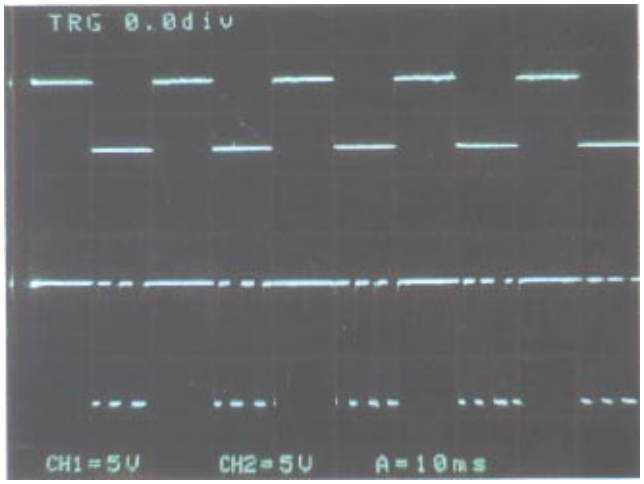

(a)

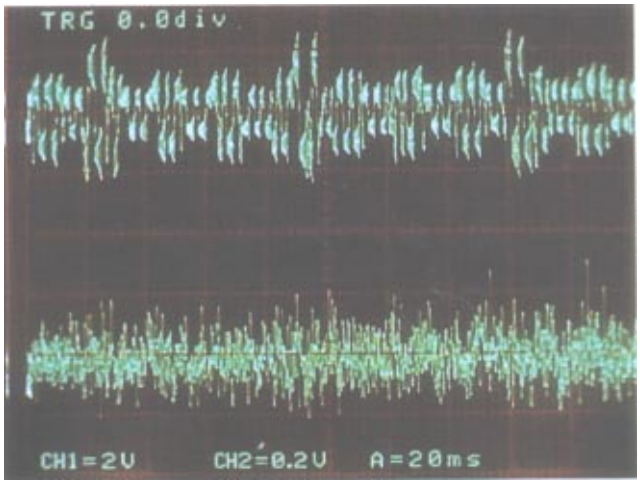

(b)

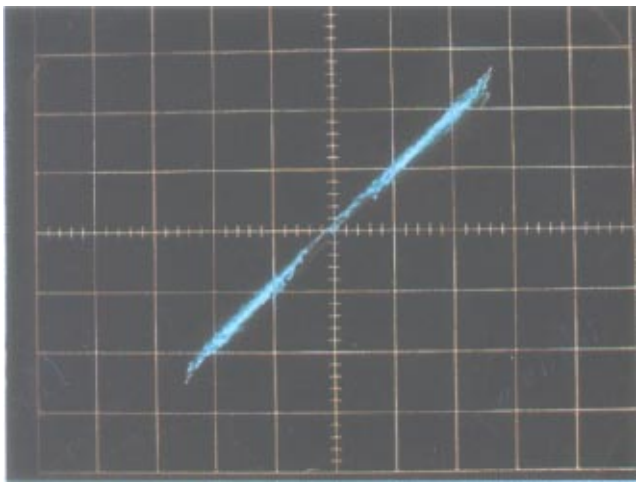

(c)

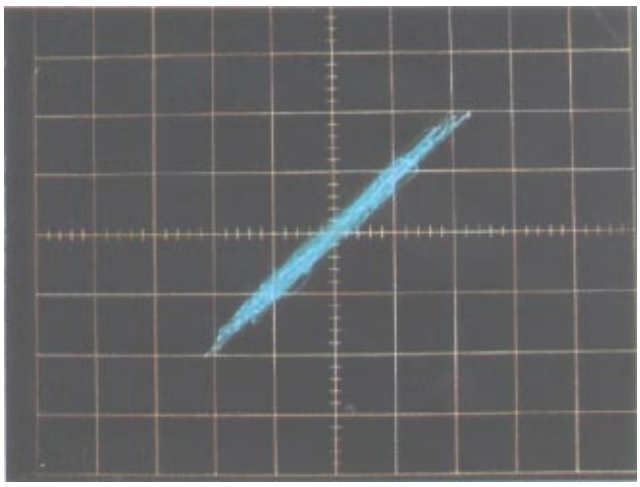

(d)

Fig. 30. Experimental results on robustness of spread spectrum communication systems to additive channel noise. The voltage $v_1(t)$ of Chua's oscillator is chosen as the chaotic spreading carrier and DS modulation is used. $Q/T = 10\%$, $T = 20$ μs. (a) The binary message signal $s(t)$ (the upper trace) and the recovered message signal $r(t)$ (the lower trace). (b) Transmitted signal (the upper trace) and additive channel noise (the lower trace). (c) Oscilloscope trace of v_1–v_1' plane. (d) Oscilloscope trace of v_2–v_2' plane.

shows the triangular message signal and the recovered message signal. Figure 27(b) shows the binary message signal and the recovered message signal. Figure 27(c) shows the transmitted signal, which consists of both synchronization impulses and the modulated message signal.

The experimental results for the DS modulation when hyperchaotic circuits are used are shown in Fig. 29. The message signal $s(t)$ is modulated by $(v_2(t) - v_1(t))$; namely, the modulated message signal is $(v_2(t) - v_1(t))s_1(t)$. Conditions are given by: $Q/T = 34\%$ and $T = 2.5 \times 10^{-6}$ s. Figure 29(a) shows the triangular message signal and the recovered message signal. Figure 29(b) shows the binary message signal and the recovered message signal. Figure 29(c) shows the transmitted signal, which consists of both synchronization impulses and the modulated message signal.

From the above experimental results we conclude that both chaotic spread spectrum communication systems work well. We also conclude that impulsive synchronization is useful for

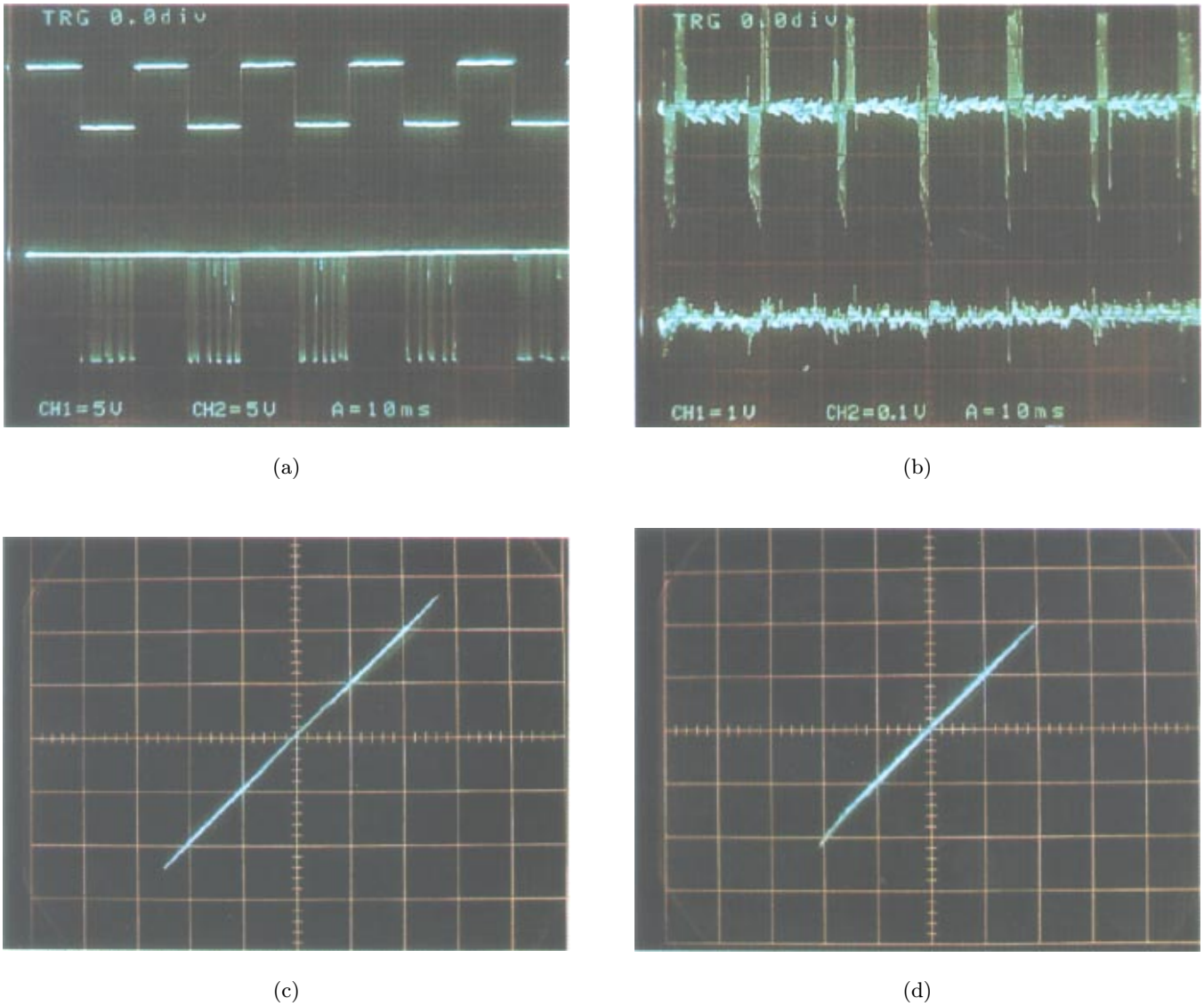

(a) (b)

(c) (d)

Fig. 31. Experimental results on robustness of spread spectrum communication systems to additive channel noise. The voltage $v_2(t)$ of Chua's oscillator is chosen as the chaotic spreading carrier and DS modulation is used. $Q/T = 10\%$, $T = 20$ μs. (a) The binary message signal $s(t)$ (the upper trace) and the recovered message signal $r(t)$ (the lower trace). (b) Transmitted signal (the upper trace) and additive channel noise (the lower trace). (c) Oscilloscope trace of v_1–v_1' plane. (d) Oscilloscope trace of v_2–v_2' plane.

synchronizing chaotic systems in the transmitter and the receiver even though Q is not small.

We have also evaluated the robustness of chaotic spread spectrum communication systems based on impulsive synchronization by adding noise into the communication channel. Only cases when the message signals are binary are studied in our experiments. Figures 30 and 31 show experimental results when Chua's oscillators and DS modulations are used. Figure 30 shows the results when the chaotic spreading carrier is $v_1(t)$. Figure 30(a) shows the binary message signal and the recovered message signal. Observe that the result can be easily improved by low-pass filtering and thresholding. The channel noise is shown in Fig. 30(b). Observe that the amplitude of the additive channel noise is around 1/10 of that of the transmitted signal. Figures 30(c) and 30(d) show the oscilloscope traces on the v_1–v_1' and v_2–v_2' planes, respectively. Observe that the synchronization error is small.

Figure 31 shows the results when the chaotic spreading carrier is $v_2(t)$. Figure 31(a) shows the binary message signal and the recovered message signal. This result can also be improved by

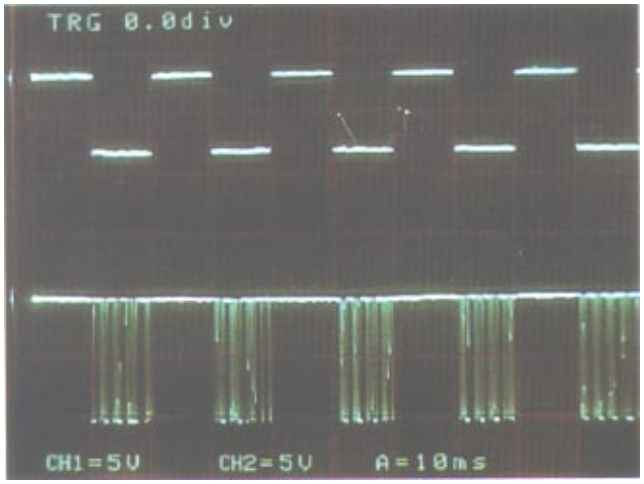

(a)

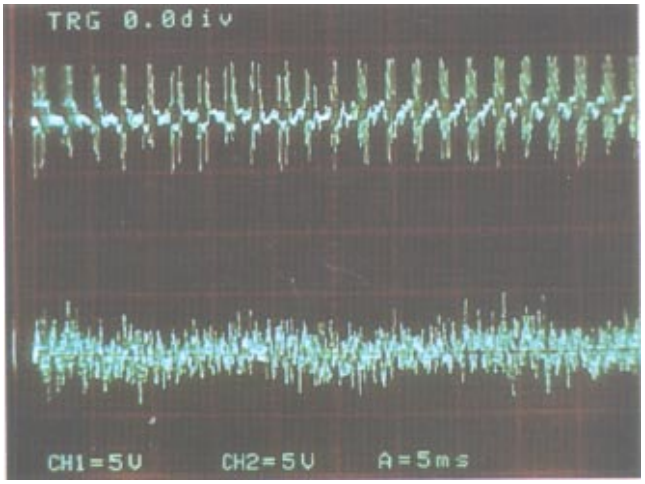

(b)

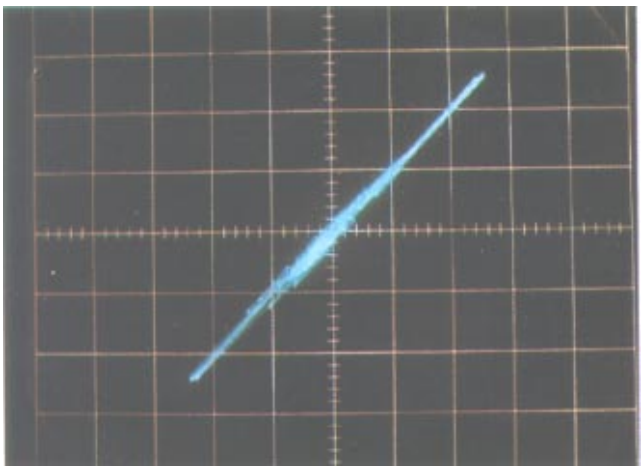

(c)

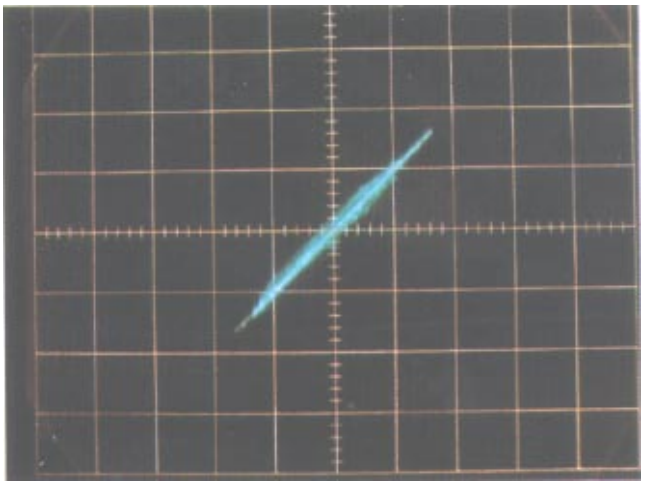

(d)

Fig. 32. Experimental results on robustness of spread spectrum communication systems to additive channel noise. The voltage $v_2(t)$–$v_1(t)$ of the hyperchaotic circuit is chosen as the chaotic spreading carrier and DS modulation is used. $Q/T = 34\%$, $T = 2.5$ μs. (a) The binary message signal $s(t)$ (the upper trace) and the recovered message signal $r(t)$ (the lower trace). (b) Transmitted signal (the upper trace) and additive channel noise (the lower trace). (c) Oscilloscope trace of v_1–v_1' plane. (d) Oscilloscope trace of v_2–v_2' plane.

low-pass filtering and thresholding. The channel noise is shown in Fig. 31(b). Observe that the amplitude of the additive channel noise is around 1/10 of that of the chaotic spreading carrier. Figures 31(c) and 31(d) show the oscilloscope traces on the v_1–v_1' and v_2–v_2' planes, respectively. Observe that the synchronization error is small.

Figure 32 shows experimental results when the hyperchaotic circuits and DS modulations are used. The chaotic spreading carrier is $v_2(t)$–$v_1(t)$. Figure 32(a) shows the binary message signal and the recovered message signal. We can easily improve the recovered results by low-pass filtering and thresholding. The channel noise is shown in Fig. 32(b). In this case, the amplitude of the noise is almost 1/2 of that of the transmitted signal. Figure 32(c) and 32(d) show the oscilloscope traces on the v_1–v_1' and v_2–v_2' planes, respectively. Observe that the synchronization error is small.

From our experiments we found that the binary message signal can be completely recovered if the SNR is around 12 dB. In this case, the 45-degree lines become very thick. This means that we can recover the binary information signal even if

the synchronization is far from the desired almost-identical synchronization. Furthermore, if we use some error-correction coding techniques, the binary message signal can be completely recovered even under a low SNR.

4. Concluding Remarks

We have presented a series of experimental results on the impulsive synchronizations between two Chua's oscillators and two hyperchaotic circuits. Our experimental results show that the impulsive synchronization is very robust to both parameter mismatch and channel noise. We have also found that the performance of impulsive synchronization depends heavily on the frequency and the width of the synchronization impulses. We have presented our experimental results on chaotic spread spectrum communication systems based on impulsive synchronizations. Our experimental results show that both additive modulation and DS modulation are robust enough to channel noise. Our experimental results also suggest that impulsive synchronization is a promising approach in the design of practical chaotic spread spectrum communication systems.

Acknowledgment

This work is supported in part by the Office of Naval Research(ONR) under grant numbers N00014-97-1-0463 and N00014-96-1-0753.

References

Chua, L. O., Kocarev, L., Eckert, K. & Itoh, M. [1992] "Experimental chaos synchronization in Chua's circuit," *Int. J. Bifurcation and Chaos* **2**(3), 705–708.

Chua, L. O., Itoh, M., Kocarev, L. & Eckert, K. [1993] "Chaos synchronization in Chua's circuit," *J. Circuits Syst. Comput.* **3**(1), 93–108.

Dedieu, H., Kennedy, M. & Hasler, M. [1993] "Chaos shift keying: Modulation and demodulation of a chaotic carrier using self-synchronizing Chua's circuits," *IEEE Trans. Circuits Syst.* **CAS-40**(10), 643–642.

Halle, K. S., Wu C. W., Itoh, M. & Chua, L. O. [1992] "Spread spectrum communication through modulation of chaos," *Int. J. Bifurcation and Chaos* **3**(2), 469–477.

Itoh, M. & Murakami, H. [1995] "New communication systems via chaotic synchronizations and modulations," *IEICE Trans. Fundamentals* **E78-A**(3), 285–290.

Itoh, M. [1999] "Spread spectrum communication via chaos," *Int. J. Bifurcation and Chaos* **9**(1), 155–213.

Kocarev, L., Halle, K. S., Eckert, K., Chua, L. O. & Parlitz, U. [1992] "Experimental demonstration of secure communications via chaotic synchronization," *Int. J. Bifurcation and Chaos* **2**(3), 709–713.

Lipton, J. M. & Dabke, K. P. [1996] "Spread spectrum communications based on chaotic systems," *Int. J. Bifurcation and Chaos* **6**(12A), 2361–2374.

Madan, R. [1993] *Chua's Circuit: A Paradigm for Chaos* (World Scientific, Singapore).

Matsumoto, T., Chua, L. O. & Kobayashi, K. [1986] "Hyperchaos: Laboratory experiment and numerical confirmation," *IEEE Trans. Circuits Syst.* **CAS-33**(11), 1143–1147.

Panas, A. I., Yang, T. & Chua, L. O. [1998] "Experimental results of impulsive synchronization between two Chua's circuits," *Int. J. Bifurcation and Chaos* **8**(3), 639–644.

Parlitz, U., Chua, L. O., Kocarev, L., Halle, S. & Shang, A. [1992] "Transmission of digital signals by chaotic synchronization," *Int. J. Bifurcation and Chaos* **2**(4), 973–977.

Parlitz, U. & Ergezinger, S. [1994] "Robust communication based on chaotic spreading sequences," *Phys. Lett.* **A188**, 146–150.

Pecora, L. & Carroll, T. [1990] "Synchronization in chaotic systems, " *Phys. Rev. Lett.* **64**(8), 821–824.

Yang, T. & Chua, L. O. [1997a] "Impulsive control and synchronization of nonlinear dynamical systems and application to secure communication," *Int. J. Bifurcation and Chaos* **7**(3), 645–664.

Yang, T. & Chua, L. O. [1997b] "Chaotic digital code-division multiple access (CDMA) communication systems," *Int. J. Bifurcation and Chaos* **7**(12), 2789–2805.

Yang, T. & Chua, L. O. [1997c] "Impulsive stabilization for control and synchronization of chaotic systems: Theory and application to secure communication," *Trans. Circuits Syst. I* **44**(10), 976–988.

Yang, T. & Chua, L. O. [1998a] "Applications of chaotic digital code-division multiple access (CDMA) to cable communication systems," *Int. J. Bifurcation and Chaos* **8**(8), 1657–1669.

Yang, T. & Chua, L. O. [1998b] "Error performance of chaotic digital code-division multiple access (CDMA) systems," *Int. J. Bifurcation and Chaos* **8**(10), 2047–2059.